

# Data-driven Implementations of Various Generalizations of Balanced Truncation

Umair Zulfiqar<sup>a,\*</sup>

<sup>a</sup>*School of Electronic Information and Electrical Engineering, Yangtze University, Jingzhou, Hubei, 434023, China*

---

## Abstract

There exist two main frameworks for non-intrusive implementations of approximate balanced truncation: the quadrature-based framework [1] and the ADI-based framework [2]. Both approaches rely solely on samples of the transfer function to construct truncated balanced models, eliminating the need for access to the original model's state-space realization. Recently, the quadrature-based framework has been extended to various generalizations of balanced truncation, including positive-real balanced truncation, bounded-real balanced truncation, and balanced stochastic truncation. While this extension [3] is theoretically non-intrusive—meaning it does not require the original state-space realization—it depends on samples of spectral factorizations of the transfer function. Since practical methods for obtaining such samples are currently unavailable, this extension remains largely a theoretical contribution.

In this work, we present a non-intrusive ADI-type framework for these generalized balanced truncation methods that requires only samples of the original transfer function for implementation. To achieve this, we first demonstrate how the approximations of ADI-type method for Riccati equations (RADI) [4] can be equivalently obtained via projection-based interpolation. Leveraging this insight, we develop several non-intrusive, data-driven algorithms that not only satisfy the desired interpolation conditions but also preserve key system prop-

---

\*Corresponding author

*Email address:* [umairzulfiqar@shu.edu.cn](mailto:umairzulfiqar@shu.edu.cn) (Umair Zulfiqar)

erties such as positive-realness, bounded-realness, and minimum phase. Notably, these algorithms rely solely on solving Lyapunov and Sylvester equations, avoiding computationally intensive Riccati equations or linear matrix inequalities. Additionally, we propose non-intrusive, data-driven implementations of RADI (and ADI)-based generalizations of balanced truncation, covering LQG balanced truncation,  $\mathcal{H}_\infty$  balanced truncation, positive-real balanced truncation, bounded-real balanced truncation, self-weighted balanced truncation, and balanced stochastic truncation. We also discuss practical considerations for improving computational efficiency. Numerical experiments demonstrate that the proposed algorithms perform comparably to their intrusive counterparts.

*Keywords:* ADI, Balanced truncation, Data-driven, Low-rank, Non-intrusive

---

## 1. Preliminaries

Consider a stable  $n^{\text{th}}$ -order linear time-invariant (LTI) system  $G(s)$ , represented in minimal state-space form as

$$G(s) = C(sI - A)^{-1}B + D,$$

with matrices  $A \in \mathbb{R}^{n \times n}$ ,  $B \in \mathbb{R}^{n \times m}$ ,  $C \in \mathbb{R}^{p \times m}$ , and  $D \in \mathbb{R}^{p \times m}$ .

Consider an  $r^{\text{th}}$ -order stable reduced-order approximation  $\hat{G}(s)$  of  $G(s)$  with minimal state-space realization:

$$\hat{G}(s) = \hat{C}(sI - \hat{A})^{-1}\hat{B} + D,$$

where  $\hat{A} \in \mathbb{C}^{r \times r}$ ,  $\hat{B} \in \mathbb{C}^{r \times m}$ ,  $\hat{C} \in \mathbb{C}^{p \times r}$ , and  $r \ll n$ .

The reduced-order model ROM  $\hat{G}(s)$  is constructed from  $G(s)$  through Petrov-Galerkin projection:

$$\hat{A} = \hat{W}^* A \hat{V}, \quad \hat{B} = \hat{W}^* B, \quad \hat{C} = C \hat{V},$$

using full-rank projection matrices  $\hat{V}, \hat{W} \in \mathbb{C}^{n \times r}$  satisfying  $\hat{W}^* \hat{V} = I$ . Importantly, the ROM remains unchanged under transformations  $\hat{V} \rightarrow \hat{V} T_v$  and  $\hat{W} \rightarrow \hat{W} T_w$ , where  $T_v, T_w \in \mathbb{C}^{r \times r}$  are nonsingular. This property allows the

complex projection matrices  $(\hat{V}, \hat{W})$  and corresponding reduced-order state-space matrices  $(\hat{A}, \hat{B}, \hat{C})$  to be converted to real-valued representations through appropriate similarity transformations [5].

### 1.1. Interpolation Theory [6]

Consider the right interpolation points  $(\sigma_1, \dots, \sigma_v)$  and left interpolation points  $(\mu_1, \dots, \mu_w)$ . In the interpolation framework, the projection matrices  $\hat{V} \in \mathbb{C}^{n \times vm}$  and  $\hat{W} \in \mathbb{C}^{n \times wp}$  are constructed as:

$$\hat{V} = \begin{bmatrix} (\sigma_1 I - A)^{-1} B & \dots & (\sigma_v I - A)^{-1} B \end{bmatrix}, \quad (1)$$

$$\hat{W} = \begin{bmatrix} (\mu_1^* I - A^T)^{-1} C^T & \dots & (\mu_w^* I - A^T)^{-1} C^T \end{bmatrix}. \quad (2)$$

To enforce the Petrov-Galerkin condition  $(\hat{W}^* \hat{V} = I)$ ,  $\hat{W}$  is replaced with  $\hat{W} T_w$ , where  $T_w = (\hat{V}^* \hat{W})^{-1}$ . The resulting ROM satisfies the interpolation conditions:

$$G(\sigma_i) = G_r(\sigma_i), \quad G(\mu_i) = G_r(\mu_i). \quad (3)$$

Additionally, if there are common right and left interpolation points, i.e.,  $\sigma_i = \mu_j$ , the following Hermite interpolation conditions are also satisfied for those points:

$$G'(\sigma_i) = G'_r(\sigma_i). \quad (4)$$

### 1.2. Interpolatory Loewner framework [7]

The matrix  $D$  can be obtained by sampling the transfer function  $G(s)$  at a sufficiently high frequency, since  $D = \lim_{s \rightarrow \infty} G(s)$ . Let  $H(s)$  be defined as:

$$H(s) = C(sI - A)^{-1} B.$$

Samples of  $H(s_i)$  can be computed from those of  $G(s_i)$  as:

$$H(s_i) = G(s_i) - G(\infty).$$

In the Loewner framework, the following matrices are constructed from  $H(s)$  samples at interpolation points:

$$\begin{aligned}
\hat{W}^* \hat{V} &= \begin{bmatrix} -\frac{H(\sigma_1) - H(\mu_1)}{\sigma_1 - \mu_1} & \dots & -\frac{H(\sigma_v) - H(\mu_1)}{\sigma_v - \mu_1} \\ \vdots & \ddots & \vdots \\ -\frac{H(\sigma_1) - H(\mu_w)}{\sigma_1 - \mu_w} & \dots & -\frac{H(\sigma_v) - H(\mu_w)}{\sigma_v - \mu_w} \end{bmatrix}, \\
\hat{W}^* A \hat{V} &= \begin{bmatrix} -\frac{\sigma_1 H(\sigma_1) - \mu_1 H(\mu_1)}{\sigma_1 - \mu_1} & \dots & -\frac{\sigma_v H(\sigma_v) - \mu_1 H(\mu_1)}{\sigma_v - \mu_1} \\ \vdots & \ddots & \vdots \\ -\frac{\sigma_1 H(\sigma_1) - \mu_w H(\mu_w)}{\sigma_1 - \mu_w} & \dots & -\frac{\sigma_v H(\sigma_v) - \mu_w H(\mu_w)}{\sigma_v - \mu_w} \end{bmatrix}, \\
\hat{W}^* B &= \begin{bmatrix} H(\mu_1) \\ \vdots \\ H(\mu_w) \end{bmatrix}, \quad \hat{C} = C \hat{V} = [H(\sigma_1) \dots H(\sigma_v)], \tag{5}
\end{aligned}$$

where  $\hat{V}$  and  $\hat{W}$  are as defined in (1) and (2), respectively. When  $\sigma_j \approx \mu_i$ ,

$$\begin{aligned}
\frac{H(\sigma_j) - H(\mu_i)}{\sigma_j - \mu_i} &\approx H'(\sigma_j), \\
\frac{\sigma_j H(\sigma_j) - \mu_i H(\mu_i)}{\sigma_j - \mu_i} &\approx H(\sigma_j) + \sigma_j H'(\sigma_j).
\end{aligned}$$

Thus, if the sets of right and left interpolation points share common elements, derivative samples  $H'(\sigma_j)$  are also needed to construct  $\hat{W}^* \hat{V}$  and  $\hat{W}^* A \hat{V}$ . The matrices  $\hat{W}^* \hat{V}$  and  $\hat{W}^* A \hat{V}$  exhibit a special structure known as the Loewner matrix and shifted Loewner matrix, respectively, which gives the name ‘‘Interpolatory Loewner Framework’’. The matrix  $\hat{W}^* \hat{V}$  is not always invertible, preventing the computation of  $\hat{A} = (\hat{W}^* \hat{V})^{-1} \hat{W}^* A \hat{V}$  and  $\hat{B} = (\hat{W}^* \hat{V})^{-1} \hat{W}^* B$ . Instead, the ROM is constructed in descriptor form:

$$\hat{G}(s) = C \hat{V} (s \hat{W}^* \hat{V} - \hat{W}^* A \hat{V})^{-1} \hat{W}^* B + G(\infty).$$

### 1.3. Pseudo-optimal Rational Krylov Algorithm [8]

The matrices  $S_v$ ,  $S_w$ ,  $L_v$ , and  $L_w$  are defined as:

$$\begin{aligned}
S_v &= \text{diag}(\sigma_1, \dots, \sigma_r) \otimes I_m, & S_w &= \text{diag}(\mu_1, \dots, \mu_r) \otimes I_m, \\
L_v &= [1, \dots, 1] \otimes I_m, & L_w^T &= [1, \dots, 1] \otimes I_m. \tag{6}
\end{aligned}$$

The projection matrices  $\hat{V}$  and  $\hat{W}$  in (1) and (2) solve:

$$A \hat{V} - \hat{V} S_v + B L_v = 0, \tag{7}$$

$$A^T \hat{W} - \hat{W} S_w^* + C^T L_w^T = 0. \tag{8}$$

Pre-multiplying (7) with  $\hat{W}^*$  under the condition  $\hat{W}^*\hat{V} = I$  reveals that  $\hat{A} = S_v - \hat{B}L_v$ . This parameterizes  $A_r$  in terms of  $\hat{B} = \zeta$  while preserving the interpolation conditions induced by  $\hat{V}$ , i.e., varying  $\zeta$  is equivalent to varying  $\hat{W}$ .

Let us assume that all interpolation points  $(\sigma_1, \dots, \sigma_v)$  lie in the right half of the  $s$ -plane. Consider the observable pair  $(S_v, L_v)$  that satisfies the Lyapunov equation:

$$-S_v^*Q_v - Q_vS_v + L_v^TL_v = 0. \quad (9)$$

With the free parameter  $\zeta = Q_v^{-1}L_v^T$ , we obtain  $\hat{A} = S_v - \hat{B}L_v = -Q_v^{-1}S_v^*Q_v$ . The resulting ROM

$$\hat{A}_r = -Q_v^{-1}S_v^*Q_v, \quad \hat{B} = Q_v^{-1}L_v^T, \quad \hat{C} = CV,$$

meets the  $\mathcal{H}_2$ -optimality condition  $\frac{\partial}{\partial \zeta}(\|G(s) - \hat{G}(s)\|_{\mathcal{H}_2}^2)$ . This method is referred to as Input PORK (I-PORK) throughout this paper.

Similarly, pre-multiplying (8) with  $\hat{V}^*$  shows that  $\hat{A}$  can also be expressed as  $\hat{A} = S_w - L_w\hat{C}$ . This parameterizes  $\hat{A}$  in terms of  $\hat{C} = \zeta$  while preserving the interpolation conditions induced by  $\hat{W}$ , since changing  $\zeta$  is equivalent to varying  $\hat{V}$ .

Let us assume that all interpolation points  $(\mu_1, \dots, \mu_w)$  lie in the right half of the  $s$ -plane. For the controllable pair  $(S_w, L_w)$  that satisfies the Lyapunov equation:

$$-S_wP_w - P_wS_w^* + L_wL_w^T = 0, \quad (10)$$

choosing the free parameter  $\zeta = L_w^TP_w^{-1}$  leads to the expression  $\hat{A} = S_w - L_w\hat{C} = -P_wS_w^*P_w^{-1}$ . The resulting ROM

$$\hat{A} = -P_wS_w^*P_w^{-1}, \quad \hat{B} = \hat{W}^*B, \quad \hat{C} = L_w^TP_w^{-1}, \quad (11)$$

satisfies the  $\mathcal{H}_2$ -optimality condition given by  $\frac{\partial}{\partial \zeta}(\|G(s) - \hat{G}(s)\|_{\mathcal{H}_2}^2)$ . This approach is referred to as Output PORK (O-PORK) throughout this paper.

#### 1.4. Balanced Truncation Family

The controllability Gramian  $P$  and observability Gramian  $Q$  are defined through the frequency-domain integrals:

$$P = \frac{1}{2\pi} \int_{-\infty}^{\infty} (j\omega I - A)^{-1} B B^T (-j\omega I - A^T)^{-1} d\omega, \quad (12)$$

$$Q = \frac{1}{2\pi} \int_{-\infty}^{\infty} (-j\omega I - A^T)^{-1} C^T C (j\omega I - A)^{-1} d\omega. \quad (13)$$

These Gramians solve the following Lyapunov equations:

$$AP + PA^T + BB^T = 0, \quad (14)$$

$$A^T Q + QA + C^T C = 0. \quad (15)$$

The Cholesky factorizations of the Gramians are given by

$$P = L_p L_p^T \quad \text{and} \quad Q = L_q L_q^T.$$

The balanced square-root algorithm (BSA) [9] is among the most numerically stable methods for implementing balanced truncation (BT) [10]. It begins by computing the singular value decomposition (SVD) of the product  $L_q^T L_p$ :

$$L_q^T L_p = \begin{bmatrix} U_1 & U_2 \end{bmatrix} \begin{bmatrix} \Sigma_r & 0 \\ 0 & \Sigma_{n-r} \end{bmatrix} \begin{bmatrix} V_1^T \\ V_2^T \end{bmatrix}.$$

The projection matrices  $\hat{W}$  and  $\hat{V}$  in BSA are constructed as:

$$\hat{W} = L_q U_1 \Sigma_r^{-\frac{1}{2}} \quad \text{and} \quad \hat{V} = L_p V_1 \Sigma_r^{-\frac{1}{2}}.$$

The ROM constructed by BT preserves the stability of the original system  $G(s)$  as well as its  $r$  largest Hankel singular values  $\sqrt{\lambda_i(PQ)}$ . To preserve additional properties—such as stable minimum phase, positive-realness, or bounded-realness—generalized versions of BT have been developed, which primarily differ in their definitions of the Gramians.

In Linear Quadratic Gaussian (LQG) BT (LQG-BT) [11], the Gramian-like matrices are computed by solving the following filter and controller Riccati

equations:

$$AP_{\text{LQG}} + P_{\text{LQG}}A^T + BB^T - P_{\text{LQG}}C^T CP_{\text{LQG}} = 0, \quad (16)$$

$$A^T Q_{\text{LQG}} + Q_{\text{LQG}}A^T + C^T C - Q_{\text{LQG}}BB^T Q_{\text{LQG}} = 0. \quad (17)$$

By replacing  $P$  and  $Q$  with  $P_{\text{LQG}}$  and  $Q_{\text{LQG}}$  in BT, respectively, a ROM can be obtained that is suitable for designing a reduced-order LQG controller with good closed-loop performance when used with the original plant.

In  $\mathcal{H}_\infty$  BT ( $\mathcal{H}_\infty$ -BT) [12], the Gramian-like matrices are computed by solving the following filter and controller Riccati equations with  $\gamma > 0$ :

$$AP_{\mathcal{H}_\infty} + P_{\mathcal{H}_\infty}A^T + BB^T - (1 - \gamma^{-2})P_{\mathcal{H}_\infty}C^T CP_{\mathcal{H}_\infty} = 0, \quad (18)$$

$$A^T Q_{\mathcal{H}_\infty} + Q_{\mathcal{H}_\infty}A^T + C^T C - (1 - \gamma^{-2})Q_{\mathcal{H}_\infty}BB^T Q_{\mathcal{H}_\infty} = 0. \quad (19)$$

By replacing  $P$  and  $Q$  with  $P_{\mathcal{H}_\infty}$  and  $Q_{\mathcal{H}_\infty}$  in BT, respectively, a ROM can be obtained that is suitable for designing a reduced-order  $\mathcal{H}_\infty$  controller with good closed-loop performance when used with the original plant.

In positive-real BT (PR-BT) [13, 14], the Gramians solve the following Riccati equations:

$$AP_{\text{PR}} + P_{\text{PR}}A^T + (B - P_{\text{PR}}C^T)(D + D^T)^{-1}(B - P_{\text{PR}}C^T)^T = 0, \quad (20)$$

$$A^T Q_{\text{PR}} + Q_{\text{PR}}A + (C - B^T Q_{\text{PR}})^T (D + D^T)^{-1}(C - B^T Q_{\text{PR}}) = 0. \quad (21)$$

By replacing  $P$  and  $Q$  with  $P_{\text{PR}}$  and  $Q_{\text{PR}}$  in BT, respectively, a ROM that preserves the positive-realness of the original model can be obtained.

In bounded-real BT (BR-BT) [15, 14], the Gramians solve the following Riccati equations:

$$AP_{\text{BR}} + P_{\text{BR}}A^T + BB^T + (P_{\text{BR}}C^T + BD^T)(I - DD^T)^{-1} \\ \times (P_{\text{BR}}C^T + BD^T)^T = 0, \quad (22)$$

$$A^T Q_{\text{BR}} + Q_{\text{BR}}A + C^T C + (B^T Q_{\text{BR}} + D^T C)^T (I - D^T D)^{-1} \\ \times (B^T Q_{\text{BR}} + D^T C) = 0. \quad (23)$$

By replacing  $P$  and  $Q$  with  $P_{\text{BR}}$  and  $Q_{\text{BR}}$  in BT, respectively, a ROM that preserves the bounded-realness of the original model can be obtained.

In self-weighted BT (SW-BT) [16], the controllability Gramian  $P$  remains the same as in BT, while the weighted observability Gramian  $Q_{\text{SW}}$  solves the following Lyapunov equation:

$$(A - BD^{-1}C)^T Q_{\text{SW}} + Q_{\text{SW}}(A - BD^{-1}C) + C^T(DD^T)^{-1}C = 0. \quad (24)$$

By replacing  $Q$  with  $Q_{\text{SW}}$  in BT, a ROM that preserves the minimum-phase property of the original model can be obtained.

In balanced stochastic truncation (BST) [13, 17], the controllability Gramian  $P$  remains the same as in BT, while the weighted observability Gramian  $Q_{\text{S}}$  solves the following Riccati equation:

$$\begin{aligned} A^T Q_{\text{S}} + Q_{\text{S}} A + (C - (CP + DB^T)Q_{\text{S}})^T (DD^T)^{-1} \\ \times (C - (CP + DB^T)Q_{\text{S}}) = 0. \end{aligned} \quad (25)$$

By replacing  $Q$  with  $Q_{\text{S}}$  in BT, a ROM that preserves the minimum-phase property of the original model can be obtained. Unlike SW-BT, BST can handle non-minimum-phase models as well. Both SW-BT and BST minimize the relative error  $G^{-1}(s)(G(s) - \hat{G}(s))$  and tend to ensure uniform accuracy across the entire frequency spectrum.

### 1.5. Quadrature-based Non-intrusive Implementation of Balanced Truncation

The integrals (12) and (13) can be approximated numerically using quadrature rules as:

$$\begin{aligned} P &\approx \tilde{P} = \sum_{i=1}^{n_p} w_{p,i}^2 (j\omega_i I - A)^{-1} B B^T (-j\omega_i I - A^T)^{-1}, \\ Q &\approx \tilde{Q} = \sum_{i=1}^{n_q} w_{q,i}^2 (-j\nu_i I - A^T)^{-1} C^T C (j\nu_i I - A)^{-1}, \end{aligned}$$

where  $\omega_i$  and  $\nu_i$  are the quadrature nodes, and  $w_{p,i}^2$  and  $w_{q,i}^2$  are their corresponding weights. The factorizations  $\tilde{P} = \tilde{L}_p \tilde{L}_p^T$  and  $\tilde{Q} = \tilde{L}_q \tilde{L}_q^T$  can be expressed as:

$\tilde{L}_p = \hat{V}\hat{L}_p$  and  $\tilde{L}_q = \hat{W}\hat{L}_q$ , with

$$\hat{V} = \begin{bmatrix} (j\omega_1 I - A)^{-1}B & \cdots & (j\omega_{n_p} I - A)^{-1}B \end{bmatrix}, \quad (26)$$

$$\hat{W} = \begin{bmatrix} (-j\nu_1 I - A^T)^{-1}C^T & \cdots & (-j\nu_{n_q} I - A^T)^{-1}C^T \end{bmatrix}, \quad (27)$$

$$\hat{L}_p = \text{diag}(w_{p,1}, \dots, w_{p,n_p}) \otimes I_m,$$

$$\hat{L}_q = \text{diag}(w_{q,1}, \dots, w_{q,n_q}) \otimes I_m.$$

Here,  $\hat{L}_p$  and  $\hat{L}_q$  depend only on the quadrature weights. Moreover, the terms  $\hat{W}^*\hat{V}$ ,  $\hat{W}^*A\hat{V}$ ,  $\hat{W}^*B$ ,  $C\hat{V}$ , and  $D$  can be constructed non-intrusively using samples of  $G(s)$  via the Loewner framework. In the BSA,  $\tilde{L}_p$  and  $\tilde{L}_q$  replace  $L_p$  and  $L_q$ , leading to the decomposition:

$$\hat{L}_q^*(\hat{W}^*\hat{V})\hat{L}_p = \begin{bmatrix} \tilde{U}_1 & \tilde{U}_2 \end{bmatrix} \begin{bmatrix} \tilde{\Sigma}_r & 0 \\ 0 & \tilde{\Sigma}_{n-r} \end{bmatrix} \begin{bmatrix} \tilde{V}_1^* \\ \tilde{V}_2^* \end{bmatrix}. \quad (28)$$

The projection matrices  $W_r$  and  $V_r$  are then defined as:

$$W_r = \hat{L}_q \tilde{U}_1 \tilde{\Sigma}_r^{-1/2} \quad \text{and} \quad V_r = \hat{L}_p \tilde{V}_1 \tilde{\Sigma}_r^{-1/2}. \quad (29)$$

Finally, the ROM in Quadrature-based BT (QuadBT) [1] is constructed as:

$$\hat{A} = W_r^*(\hat{W}^*A\hat{V})V_r, \quad \hat{B} = W_r^*(\hat{W}^*B), \quad \hat{C} = (C\hat{V})V_r. \quad (30)$$

In [3], the following observations were made about PRBT, BRBT, and BST:

1. In PR-BT, the Gramians  $P_{\text{PR}}$  and  $Q_{\text{PR}}$  are respectively the controllability Gramian and observability Gramian associated with state-space realizations of the spectral factorizations of  $G(s) + G^*(s)$ .
2. In BR-BT, the Gramians  $P_{\text{BR}}$  and  $Q_{\text{BR}}$  are respectively the controllability Gramian and observability Gramian associated with state-space realizations of the spectral factorizations of  $I_m - G^*(s)G(s)$  and  $I_p - G(s)G^*(s)$ .
3. In BST, the observability Gramian  $Q_{\text{S}}$  is the frequency-weighted observability Gramian with weight associated with the spectral factorization of  $G(s)G^*(s)$ .

4. The QuadBT framework could be extended to PR-BT, BR-BT, and BST if samples were available for the spectral factorizations of  $G(s) + G^*(s)$ ,  $I_m - G^*(s)G(s)$ ,  $I_p - G(s)G^*(s)$ , and  $G(s)G^*(s)$ .
5. Practical methods to obtain these samples do not currently exist and remain as future work.

We do not discuss these generalizations in detail here because we focus on methods requiring only samples of  $G(s)$ , for which practical measurement methods exist, unlike for the spectral factorizations of  $G(s) + G^*(s)$ ,  $I_m - G^*(s)G(s)$ ,  $I_p - G(s)G^*(s)$ , and  $G(s)G^*(s)$ .

### 1.6. ADI-based Non-intrusive Implementation of Balanced Truncation

In [18], it is shown that PORK and the ADI method [19] produce identical approximations of Lyapunov equations when the ADI shifts are selected as the mirror images of the interpolation points. Consequently, the ADI-based approximation of  $P$  for the shifts  $(-\sigma_1, \dots, -\sigma_v)$  can be obtained via I-PORK as  $P \approx \tilde{P} = \hat{V}Q_v^{-1}\hat{V}^*$ . Similarly, the approximation of  $Q$  for the shifts  $(-\mu_1, \dots, -\mu_w)$  can be computed via O-PORK as  $Q \approx \tilde{Q} = \hat{W}P_w^{-1}\hat{W}^*$ . By factorizing  $Q_v^{-1} = \hat{L}_p\hat{L}_p^*$  and  $P_w^{-1} = \hat{L}_q\hat{L}_q^*$ , and defining  $\tilde{L}_p = \hat{V}\hat{L}_p$  and  $\tilde{L}_q = \hat{W}\hat{L}_q$ , the approximations  $\tilde{P}$  and  $\tilde{Q}$  can be expressed in factorized form as  $\tilde{P} = \tilde{L}_p\tilde{L}_p^*$  and  $\tilde{Q} = \tilde{L}_q\tilde{L}_q^*$ . As noted in [2], replacing  $L_p$  and  $L_q$  with  $\tilde{L}_p$  and  $\tilde{L}_q$  in BSA yields a non-intrusive implementation of BT. This is because  $\hat{L}_p$  and  $\hat{L}_q$  depend only on the interpolation points, and the quantities  $\hat{W}^*\hat{V}$ ,  $\hat{W}^*A\hat{V}$ ,  $\hat{W}^*B$ ,  $C\hat{V}$ , and  $D$  can be computed non-intrusively within the Loewner framework. Thus, the ADI-based BT algorithm can be implemented non-intrusively using transfer function samples in the right half-plane, unlike QuadBT, which requires samples along the imaginary axis.

## 2. Main Work

In this section, we present several new results on data-driven model reduction and controller design, outlined as follows:

1. Recall that the interpolant  $\hat{G}(s) = C\hat{V}(sI - S_v + \zeta L_v)^{-1}\zeta + D$  interpolates  $G(s)$  at  $(\sigma_1, \dots, \sigma_v)$ , where  $\hat{V}$  is defined in (1) and  $\zeta$  is a free parameter. We identify a specific choice of  $\zeta$  such that the RADI [4]-based approximation of  $P_{\text{LQG}}$  for ADI shifts  $(-\sigma_1, \dots, -\sigma_v)$  can be produced by solving a Lyapunov equation involving only the interpolation points  $(\sigma_1, \dots, \sigma_v)$  and the product  $C\hat{V}$ .
2. Similarly, for the interpolant  $\hat{G}(s) = \zeta(sI - S_w + L_w\zeta)^{-1}\hat{W}^*B + D$ , which interpolates  $G(s)$  at  $(\mu_1, \dots, \mu_w)$  with  $\hat{W}$  defined in (2), we provide a specific  $\zeta$  such that the RADI-based approximation of  $Q_{\text{LQG}}$  for ADI shifts  $(-\mu_1, \dots, -\mu_w)$  can be computed by solving a Lyapunov equation involving only the interpolation data  $(\mu_1, \dots, \mu_w)$  and  $\hat{W}^*B$ .
3. Using these approximations of  $P_{\text{LQG}}$  and  $Q_{\text{LQG}}$ , we develop a non-intrusive implementation of LQG-BT, which enables LQG controller design based solely on samples of the plant's transfer function  $G(s)$  in the right-half of the  $s$ -plane.
4. A similar approach is proposed for the non-intrusive implementation of  $\mathcal{H}_\infty$ -BT, which enables  $\mathcal{H}_\infty$  controller design based solely on samples of the plant's transfer function  $G(s)$  in the right-half of the  $s$ -plane.
5. The work in [20] presents linear matrix inequalities (LMIs)- and Riccati-based methods for choosing  $\zeta$  in  $\hat{G}(s) = C\hat{V}(sI - S_v + \zeta L_v)^{-1}\zeta + D$  that preserve positive-realness, bounded-realness, and minimum-phase properties. However, the formulas in [20] are intrusive since they require access to the state-space matrices  $(A, B, C, D)$ , and they are also computationally expensive. In contrast, we propose non-intrusive methods to compute  $\zeta$  in both  $\hat{G}(s) = C\hat{V}(sI - S_v + \zeta L_v)^{-1}\zeta + D$  and  $\hat{G}(s) = \zeta(sI - S_w + L_w\zeta)^{-1}\hat{W}^*B + D$  that preserve these system properties. These new formulas require only the transfer function samples and can be derived using Lyapunov and Sylvester equations (or even directly from  $G(s)$ , as discussed later).
6. We also provide non-intrusive formulas for computing  $\zeta$  in the above interpolants that yield the same approximations of  $P_{\text{PR}}, Q_{\text{PR}}, P_{\text{BR}}, Q_{\text{BR}}$ ,

$Q_S$  as those produced by RADI. Together with the approximation of  $Q_{SW}$  obtained via O-PORK, we construct non-intrusive implementations of PR-BT, BR-BT, SW-BT, and BST that rely solely on transfer function samples in the right-half of the  $s$ -plane.

### 2.1. RADI-based Non-intrusive Implementation of LQG-BT

As demonstrated in [18], the ADI method for computing the low-rank solution of  $P$  with shifts  $(-\sigma_1, \dots, -\sigma_v)$  corresponds to a Petrov-Galerkin approach. This method implicitly interpolates at  $(\sigma_1, \dots, \sigma_v)$  using the projection matrix  $\hat{V}$ , while the projection matrix  $\hat{W}$  is implicitly chosen to satisfy  $\hat{W}^* \hat{V} = I$ , ensuring that the poles of  $\hat{A}$  are placed at  $(-\sigma_1^*, \dots, -\sigma_v^*)$ . Similarly, [21] shows that the low-rank solution of  $P_{LQG}$  obtained via RADI with shifts  $(-\sigma_1, \dots, -\sigma_v)$  can be interpreted as a Petrov-Galerkin method. Here, interpolation is implicitly performed at  $(\sigma_1, \dots, \sigma_v)$  using  $\hat{V}$ , and  $\hat{W}$  is selected such that  $\hat{W}^* \hat{V} = I$ , placing the poles of  $\hat{A} - \hat{P}_{LQG} \hat{C}^* \hat{C}$  at  $(-\sigma_1^*, \dots, -\sigma_v^*)$ . The matrix  $\hat{P}_{LQG}$  solves the projected Riccati equation:

$$\hat{A} \hat{P}_{LQG} + \hat{P}_{LQG} \hat{A}^* + \hat{B} \hat{B}^* - \hat{P}_{LQG} \hat{C}^* \hat{C} \hat{P}_{LQG} = 0. \quad (31)$$

In the following theorem, we specify a choice of  $\zeta$  for the interpolant  $\hat{G}(s) = C\hat{V}(sI - S_v + \zeta L_v)^{-1} \zeta + D$  such that it places the poles of  $\hat{A} - \hat{P}_{LQG} \hat{C}^* \hat{C}$  at  $(-\sigma_1^*, \dots, -\sigma_v^*)$ , thereby yielding the same approximation as RADI.

**Theorem 2.1.** *Let  $\hat{V}$  be as defined in (1), with all interpolation points  $(\sigma_1, \dots, \sigma_v)$  located in the right half of the  $s$ -plane. Assume further that the pair  $(S_v, L_v)$  is observable and that  $Q_v > 0$  uniquely solves the Lyapunov equation:*

$$-S_v^* Q_v - Q_v S_v + L_v^T L_v + \hat{C}^* \hat{C} = 0. \quad (32)$$

Then, the ROM  $\hat{H}(s)$ , defined by

$$\hat{A} = S_v - \hat{B} L_v, \quad \hat{B} = Q_v^{-1} L_v^T, \quad \hat{C} = C \hat{V},$$

which interpolates  $H(s)$  at  $(\sigma_1, \dots, \sigma_v)$ , satisfies the following properties:

1. The matrix  $\hat{A}$  equals  $Q_v^{-1}(-S_v^* + \hat{C}^* \hat{C} Q_v^{-1})Q_v$ .
2. The solution  $\hat{P}_{LQG}$  to the projected Riccati equation (31) is  $Q_v^{-1}$ .
3. The matrix  $\hat{A} - \hat{P}_{LQG} \hat{C}^* \hat{C}$  is Hurwitz, with eigenvalues at  $(-\sigma_1^*, \dots, -\sigma_v^*)$ .

*Proof.* 1. Pre-multiplying (32) by  $Q_v^{-1}$  yields:

$$\begin{aligned} -Q_v^{-1}S_v^*Q_v - S_v + Q_v^{-1}L_v^T L_v + Q_v^{-1}\hat{C}^* \hat{C} &= 0 \\ S_v - \hat{B}L_v &= -Q_v^{-1}S_v^*Q_v + Q_v^{-1}\hat{C}^* \hat{C} \\ \hat{A} &= Q_v^{-1}(-S_v^* + \hat{C}^* \hat{C} Q_v^{-1})Q_v. \end{aligned}$$

2. Consider the expression:

$$\begin{aligned} \hat{A}Q_v^{-1} + Q_v^{-1}\hat{A}^* + \hat{B}\hat{B}^* - Q_v^{-1}\hat{C}^* \hat{C} Q_v^{-1} \\ &= -Q_v^{-1}S_v^* + Q_v^{-1}\hat{C}^* \hat{C} Q_v^{-1} - S_v Q_v^{-1} + Q_v^{-1}\hat{C}^* \hat{C} Q_v^{-1} \\ &\quad + Q_v^{-1}L_v^T L_v Q_v^{-1} - Q_v^{-1}\hat{C}^T \hat{C} Q_v^{-1} \\ &= -Q_v^{-1}S_v^* - S_v Q_v^{-1} + Q_v^{-1}L_v^T L_v Q_v^{-1} + Q_v^{-1}\hat{C}^T \hat{C} Q_v^{-1} \\ &= Q_v^{-1}(-S_v^*Q_v - Q_v S_v + L_v^T L_v + \hat{C}^* \hat{C})Q_v^{-1} \\ &= 0. \end{aligned}$$

This shows that  $Q_v^{-1}$  satisfies the projected Riccati equation (31).

3. Given  $\hat{A} = \hat{P}_{LQG}(-S_v^* + \hat{P}_{LQG} \hat{C}^* \hat{C})\hat{P}_{LQG}^{-1}$ , the eigenvalues of  $\hat{A}$  are equal to those of  $-S_v^* + \hat{P}_{LQG} \hat{C}^* \hat{C}$ . As  $-S_v^*$  is Hurwitz, the matrix  $\hat{A} - \hat{P}_{LQG} \hat{C}^* \hat{C}$  is Hurwitz with eigenvalues at  $(-\sigma_1^*, \dots, -\sigma_v^*)$ .

□

Note that  $Q_{LQG}$  is the dual of  $P_{LQG}$ . For completeness, we present the dual of Theorem 2.1 below, which produces the same approximation of  $Q_{LQG}$  as RADI when the shifts are chosen as  $(-\mu_1, \dots, -\mu_w)$ .

**Theorem 2.2.** *Let  $\hat{W}$  be as defined in (2), with all interpolation points  $(\mu_1, \dots, \mu_w)$  located in the right half of the  $s$ -plane. Assume further that the pair  $(S_w, L_w)$  is controllable and that  $P_w > 0$  uniquely solves the Lyapunov equation:*

$$-S_w P_w - P_w S_w^* + L_w L_w^T + \hat{B}\hat{B}^* = 0. \quad (33)$$

Then, the ROM  $\hat{H}(s)$ , defined by

$$\hat{A} = S_w - L_w \hat{C}, \quad \hat{B} = \hat{W}^* B, \quad \hat{C} = L_w^T P_w^{-1},$$

which interpolates  $H(s)$  at  $(\mu_1, \dots, \mu_w)$ , satisfies the following properties:

1. The matrix  $\hat{A}$  equals  $P_w(-S_w^* + P_w^{-1} \hat{B} \hat{B}^*) P_w^{-1}$ .
2. The solution  $\hat{Q}_{LQG}$  to the following projected Riccati equation

$$\hat{A}^* \hat{Q}_{LQG} + \hat{Q}_{LQG} \hat{A} + \hat{C}^* \hat{C} - \hat{Q}_{LQG} \hat{B} \hat{B}^* \hat{Q}_{LQG} = 0 \quad (34)$$

is  $P_w^{-1}$ .

3. The matrix  $\hat{A} - \hat{B} \hat{B}^* \hat{Q}_{LQG}$  is Hurwitz, with eigenvalues at  $(-\mu_1^*, \dots, -\mu_w^*)$ .

*Proof.* The proof is similar to that of Theorem 2.1 and hence omitted for brevity.  $\square$

Similar to the ADI-based non-intrusive implementation of BT, the RADI-based non-intrusive implementation of LQG-BT can be directly obtained using the results of Theorems 2.1 and 2.2. The pseudo-code for this implementation, named ‘‘Data-driven LQG-BT (DD-LQG-BT)’’, is provided in Algorithm 1.

*Remark 1.*  $\mathcal{H}_\infty$ -BT is similar to LQG-BT with the only difference being in the computation of  $Q_v$  and  $P_w$ . In  $\mathcal{H}_\infty$ -BT,  $Q_v$  and  $P_w$  are computed by solving the following Lyapunov equations:

$$-S_v^* Q_v - Q_v S_v + L_v^T L_v + (1 - \gamma^{-2}) \hat{C}^* \hat{C} = 0, \quad (35)$$

$$-S_w P_w - P_w S_w^* + L_w L_w^T + (1 - \gamma^{-2}) \hat{B} \hat{B}^* = 0. \quad (36)$$

All other steps in Algorithm 1 remain the same.

## 2.2. RADI-based Non-intrusive Implementation of PR-BT

Let us define

$$G_{PR}(s) = C_{PR}(sI - A_{PR})^{-1} B_{PR},$$

---

**Algorithm 1** DD-LQG-BT

**Input:** RADI shifts for approximating  $P_{\text{LQG}}$ :  $(-\sigma_1, \dots, -\sigma_v)$ ;  
RADI shifts for approximating  $Q_{\text{LQG}}$ :  $(-\mu_1, \dots, -\mu_w)$ ; **Data:**  
 $(H(\sigma_1), \dots, H(\sigma_v), H(\mu_1), \dots, H(\mu_w))$  and  $H'(\sigma_i)$  for  $\sigma_i = \mu_j$ ; Reduced  
order:  $r$ .

**Output:** ROM:  $(\hat{A}, \hat{B}, \hat{C})$

- 1: Compute the Loewner quadruplet  $(\hat{W}^* \hat{V}, \hat{W}^* A \hat{V}, \hat{W}^* B, C \hat{V})$  from the samples  $H(\sigma_i)$  and  $H(\mu_i)$  via (5).
  - 2: Set  $S_v, L_v, S_w, L_w$  as in (6).
  - 3: Compute  $Q_v$  and  $P_w$  by solving the Lyapunov equations (32) and (33).
  - 4: Decompose  $Q_v^{-1}$  and  $P_w^{-1}$  as  $Q_v^{-1} = \hat{L}_p \hat{L}_p^*$  and  $P_w^{-1} = \hat{L}_q \hat{L}_q^*$ .
  - 5: Compute  $\hat{V}_r$  and  $\hat{W}_r$  from (28) and (29).
  - 6: Compute  $\hat{A}, \hat{B}$ , and  $\hat{C}$  from (30).
- 

where

$$\begin{aligned} A_{\text{PR}} &= A - B_{\text{PR}} C_{\text{PR}}, & B_{\text{PR}} &= B R_{\text{PR}}^{-\frac{1}{2}}, \\ C_{\text{PR}} &= R_{\text{PR}}^{-\frac{1}{2}} C, & R_{\text{PR}} &= D + D^T. \end{aligned}$$

Further, define the ROM

$$\hat{G}_{\text{PR}}(s) = \hat{C}_{\text{PR}}(sI - \hat{A}_{\text{PR}})^{-1} \hat{B}_{\text{PR}}$$

obtained as follows:

$$\begin{aligned} \hat{A}_{\text{PR}} &= W_{\text{PR}}^* (A_{\text{PR}}) V_{\text{PR}} = W_{\text{PR}}^* (A - B R_{\text{PR}}^{-1} C) V_{\text{PR}} = \hat{A} - \hat{B} R_{\text{PR}}^{-1} \hat{C}, \\ \hat{B}_{\text{PR}} &= W_{\text{PR}}^* B_{\text{PR}} = W_{\text{PR}}^* B R_{\text{PR}}^{-\frac{1}{2}} = \hat{B} R_{\text{PR}}^{-\frac{1}{2}}, \\ \hat{C}_{\text{PR}} &= C_{\text{PR}} V_{\text{PR}} = R_{\text{PR}}^{-\frac{1}{2}} C V_{\text{PR}} = R_{\text{PR}}^{-\frac{1}{2}} \hat{C}, \end{aligned}$$

where  $W_{\text{PR}}^* V_{\text{PR}} = I$ .

The Riccati equations (20) and (21) can be rewritten as follows:

$$A_{\text{PR}} P_{\text{PR}} + P_{\text{PR}} A_{\text{PR}}^T + B_{\text{PR}} B_{\text{PR}}^T + P_{\text{PR}} C_{\text{PR}}^T C_{\text{PR}} P_{\text{PR}} = 0, \quad (37)$$

$$A_{\text{PR}}^T Q_{\text{PR}} + Q_{\text{PR}} A_{\text{PR}} + C_{\text{PR}}^T C_{\text{PR}} + Q_{\text{PR}} B_{\text{PR}} B_{\text{PR}}^T Q_{\text{PR}} = 0. \quad (38)$$

From Theorem 2.1, the RADI-based low-rank approximation of  $P_{\text{PR}}$  can be obtained as follows. The projection matrix

$$V_{\text{PR}} = \begin{bmatrix} (\sigma_1 I - A_{\text{PR}})^{-1} B_{\text{PR}} & \cdots & (\sigma_v I - A_{\text{PR}})^{-1} B_{\text{PR}} \end{bmatrix} \quad (39)$$

solves the following Sylvester equation:

$$A_{\text{PR}} V_{\text{PR}} - V_{\text{PR}} S_v + B_{\text{PR}} L_v = 0. \quad (40)$$

Then  $\hat{C}_{\text{PR}} = C_{\text{PR}} V_{\text{PR}}$  can be computed as follows:

$$\hat{C}_{\text{PR}} = \begin{bmatrix} G_{\text{PR}}(\sigma_1) & \cdots & G_{\text{PR}}(\sigma_v) \end{bmatrix}. \quad (41)$$

Thereafter,  $Q_v$  is computed by solving the Lyapunov equation:

$$-S_v^* Q_v - Q_v S_v + L_v^T L_v - \hat{C}_{\text{PR}}^* \hat{C}_{\text{PR}} = 0. \quad (42)$$

According to Theorem 2.1, the state-space realization of the ROM  $\hat{G}_{\text{PR}}(s) = \hat{C}_{\text{PR}}(sI - \hat{A}_{\text{PR}})^{-1} \hat{B}_{\text{PR}}$  (where  $\hat{A}_{\text{PR}} = S_v - Q_v^{-1} L_v^T L_v$ ,  $\hat{B}_{\text{PR}} = Q_v^{-1} L_v^T$ , and  $\hat{C}_{\text{PR}} = C_{\text{PR}} V_{\text{PR}}$ ) solves the following projected Riccati equations with  $\hat{P}_{\text{PR}} = Q_v^{-1} > 0$ :

$$\hat{A}_{\text{PR}} \hat{P}_{\text{PR}} + \hat{P}_{\text{PR}} \hat{A}_{\text{PR}}^* + \hat{B}_{\text{PR}} \hat{B}_{\text{PR}}^* + \hat{P}_{\text{PR}} \hat{C}_{\text{PR}}^* \hat{C}_{\text{PR}} \hat{P}_{\text{PR}} = 0. \quad (43)$$

Since

$$\begin{aligned} \hat{A} &= S_v - Q_v^{-1} L_v^T L_v + Q_v^{-1} L_v^T \hat{C}_{\text{PR}}, \\ \hat{B} &= Q_v^{-1} L_v^T R_{\text{PR}}^{\frac{1}{2}}, \quad \hat{C} = R_{\text{PR}}^{\frac{1}{2}} \hat{C}_{\text{PR}}, \end{aligned} \quad (44)$$

the Riccati equation (43) can be rewritten as follows:

$$\hat{A} \hat{P}_{\text{PR}} + \hat{P}_{\text{PR}} \hat{A}^* + (\hat{B} - \hat{P}_{\text{PR}} \hat{C}^*) R_{\text{PR}}^{-1} (\hat{B} - \hat{P}_{\text{PR}} \hat{C}^*)^* = 0. \quad (45)$$

The RADI-based approximation of  $P_{\text{PR}}$  is given by  $V_{\text{PR}} Q_v^{-1} V_{\text{PR}}^*$ .

**Theorem 2.3.** *Let  $G(s)$  be a positive-real transfer function. Define  $\tilde{L}_v = R_{\text{PR}}^{-\frac{1}{2}}(L_v - \hat{C}_{\text{PR}}) = \begin{bmatrix} l_{v,1} & \cdots & l_{v,v} \end{bmatrix}$  and  $T_v = \text{blkdiag}(l_{v,1}, \dots, l_{v,v})$ . Assume that:*

1. The interpolation points  $(\sigma_1, \dots, \sigma_v)$  are located in the right half of the  $s$ -plane.
2. The pair  $(S_v, \tilde{L}_v)$  is observable.
3. The matrix  $T_v$  is invertible.
4. The realization  $(\hat{A}, \hat{B}, \hat{C})$  defined in (44) is minimal.

Then the following statements hold:

1. The projection matrix  $V_{PR}$  satisfies  $V_{PR} = \hat{V}T_v$ , where  $\hat{V}$  is as in (1).
2. The ROM  $\hat{G}(s) = \hat{C}(sI - \hat{A})^{-1}\hat{B} + D$  interpolates  $G(s)$  at  $(\sigma_1, \dots, \sigma_v)$ .
3. The ROM  $\hat{G}(s)$  is positive-real.

*Proof.* By rearranging variables, the Sylvester equations (40) can be rewritten as follows:

$$AV_{PR} - V_{PR}S_v + B\tilde{L}_v = 0. \quad (46)$$

It can then readily be noted that  $V_{PR} = \hat{V}T_v$ , where  $\hat{V}$  is as in (1). Thus,  $V_{PR}$  and  $\hat{V}$  enforce the same interpolation conditions, i.e.,  $G(\sigma_i) = \hat{G}(\sigma_i)$ , since the columns of  $V_{PR}$  and  $\hat{V}$  span the same subspace and produce the same ROM with different state-space realizations [5].

By defining  $K_{PR} = (\hat{B} - \hat{P}_{PR}\hat{C}^*)R_{PR}^{-\frac{1}{2}}$ , the following holds:

$$\begin{aligned} \hat{A}\hat{P}_{PR} + \hat{P}_{PR}\hat{A}^* &= -K_{PR}K_{PR}^* \\ \hat{P}_{PR}\hat{C}^* - \hat{B} &= -K_{PR}R_{PR}^{\frac{1}{2}} \\ R_{PR}^{\frac{1}{2}}(R_{PR}^{\frac{1}{2}})^T &= D + D^T. \end{aligned} \quad (47)$$

Since  $\hat{P}_{PR} > 0$ ,  $\hat{G}(s)$  satisfies the positive-real lemma, and thus  $\hat{G}(s)$  is a positive-real transfer function [14].  $\square$

Now, assume that the matrices of the ROM  $\hat{G}_{PR}(s) = \hat{C}_{PR}(sI - \hat{A}_{PR})^{-1}\hat{B}_{PR}$  are obtained as follows:

$$\begin{aligned} \hat{A}_{PR} &= \hat{W}^*(A_{PR})\hat{V} = \hat{W}^*(A - BR_{PR}^{-1}C)\hat{V} = S_v - \zeta L_v - \zeta R_{PR}^{-1}C\hat{V}, \\ \hat{B}_{PR} &= \hat{W}^*B_{PR} = \hat{W}^*BR_{PR}^{-\frac{1}{2}} = \zeta R_{PR}^{-\frac{1}{2}}, \\ \hat{C}_{PR} &= C_{PR}\hat{V} = R_{PR}^{-\frac{1}{2}}C\hat{V}, \end{aligned} \quad (48)$$

where  $\hat{V}$  is as in (1) and  $\hat{W}$  is an unknown projection matrix satisfying  $\hat{W}^*\hat{V} = I$ . According to Theorem 2.3, the ROM  $\hat{G}_{\text{PR}}(s)$  in (48) interpolates  $G_{\text{PR}}(s)$  at the interpolation points  $(\sigma_1, \dots, \sigma_v)$  since  $V_{\text{PR}} = \hat{V}T_v$ . An immediate consequence is that a ROM  $\hat{G}_{\text{PR}}(s)$  interpolating  $G_{\text{PR}}(s)$  be constructed directly from the ROM  $\hat{G}(s) = C\hat{V}(sI - S_v + \zeta L_v)^{-1}\zeta + D$  using the formula (48). We now use this observation to derive an expression for  $T_v$ .

Note that

$$\begin{aligned}\hat{C}_{\text{PR}} &= C_{\text{PR}}V_{\text{PR}} = \begin{bmatrix} G_{\text{PR}}(\sigma_1) & \cdots & G_{\text{PR}}(\sigma_v) \end{bmatrix} = \begin{bmatrix} \hat{G}_{\text{PR}}(\sigma_1) & \cdots & \hat{G}_{\text{PR}}(\sigma_v) \end{bmatrix} \\ &= C_{\text{PR}}\hat{V} \begin{bmatrix} (\sigma_1 I - S_v + \zeta L_v + \zeta R_{\text{PR}}^{-1} C\hat{V})^{-1} \zeta R_{\text{PR}}^{-\frac{1}{2}} & \cdots & (\sigma_v I - S_v + \zeta L_v + \zeta R_{\text{PR}}^{-1} C\hat{V})^{-1} \zeta R_{\text{PR}}^{-\frac{1}{2}} \end{bmatrix} \\ &= C_{\text{PR}}\hat{V}T_v.\end{aligned}$$

It follows directly that the matrix  $T_v$  can be computed from the interpolant  $\hat{G}(s) = C\hat{V}(sI - S_v + \zeta L_v)^{-1}\zeta + D$  of  $G(s)$ . Such an interpolant can be generated by I-PORK, with guaranteed stability. Subsequently,

$$T_v = \begin{bmatrix} (\sigma_1 I - S_v + \zeta L_v + \zeta R_{\text{PR}}^{-1} C\hat{V})^{-1} \zeta R_{\text{PR}}^{-\frac{1}{2}} & \cdots & (\sigma_v I - S_v + \zeta L_v + \zeta R_{\text{PR}}^{-1} C\hat{V})^{-1} \zeta R_{\text{PR}}^{-\frac{1}{2}} \end{bmatrix}$$

can be obtained by solving the Sylvester equation:

$$(S_v - \zeta L_v - \zeta R_{\text{PR}}^{-1} C\hat{V})T_v - T_v S_v + \zeta R_{\text{PR}}^{-\frac{1}{2}} L_v = 0. \quad (49)$$

An immediate consequence is that positive-realness can be enforced non-intrusively on the ROM produced by I-PORK, using only samples of  $G(s)$  at  $\sigma_i$  and  $G(\infty)$ . This is implemented in Algorithm 2, named ‘‘Data-driven Positive-real Interpolation (V-type) (DD-PRI-V)’’. The resulting ROM is simply a different state-space realization of the ROM defined in (44).

Next, the RADI-based approximation of  $Q_{\text{PR}}$  can be obtained using Theorem 2.2 as follows. The projection matrix

$$W_{\text{PR}}^* = \begin{bmatrix} C_{\text{PR}}(\mu_1 I - A_{\text{PR}})^{-1} \\ \vdots \\ C_{\text{PR}}(\mu_w I - A_{\text{PR}})^{-1} \end{bmatrix} \quad (50)$$

---

**Algorithm 2** DD-PRI-V
 

---

**Input:** Interpolation points:  $(\sigma_1, \dots, \sigma_v)$ ; Data:  $(H(\sigma_1), \dots, H(\sigma_v))$  and  $G(\infty)$ .

**Output:** ROM:  $(\hat{A}, \hat{B}, \hat{C}, D)$

- 1: Compute  $\hat{C} = C\hat{V}$  from the samples  $H(\sigma_i)$  via (5).
  - 2: Set  $D = G(\infty)$  and  $R_{\text{PR}} = D + D^T$ .
  - 3: Set  $S_v$  and  $L_v$  as in (6).
  - 4: Compute  $Q_v$  by solving the Lyapunov equation (9).
  - 5: Compute  $T_v$  by solving the following Sylvester equation:
 
$$(S_v - Q_v^{-1}L_v^T L_v - Q_v^{-1}L_v^T R_{\text{PR}}^{-1}\hat{C})T_v - T_v S_v + Q_v^{-1}L_v^T R_{\text{PR}}^{-\frac{1}{2}}L_v = 0.$$
  - 6: Set  $\hat{C}_{\text{PR}} = R_{\text{PR}}^{-\frac{1}{2}}\hat{C}T_v$ .
  - 7: Update  $Q_v$  by solving the Lyapunov equations (42).
  - 8: Set  $\hat{B} = T_v Q_v^{-1}L_v^T R_{\text{PR}}^{\frac{1}{2}}$  and  $\hat{A} = S_v - \hat{B}L_v$ .
- 

solves the Sylvester equation:

$$A_{\text{PR}}^T W_{\text{PR}} - W_{\text{PR}} S_w^* + C_{\text{PR}}^T L_w^T = 0. \quad (51)$$

Then,  $\hat{B}_{\text{PR}} = W_{\text{PR}}^* B_{\text{PR}}$  can be computed as:

$$\hat{B}_{\text{PR}} = \begin{bmatrix} G_{\text{PR}}(\mu_1) \\ \vdots \\ G_{\text{PR}}(\mu_w) \end{bmatrix}. \quad (52)$$

Subsequently,  $P_w$  is obtained by solving the Lyapunov equation:

$$-S_w P_w - P_w S_w^* + L_w L_w^T - \hat{B}_{\text{PR}} \hat{B}_{\text{PR}}^* = 0. \quad (53)$$

According to Theorem 2.2, the state-space realization of the ROM  $\hat{G}_{\text{PR}}(s) = \hat{C}_{\text{PR}}(sI - \hat{A}_{\text{PR}})^{-1}\hat{B}_{\text{PR}}$  (where  $\hat{A}_{\text{PR}} = S_w - L_w L_w^T P_w^{-1}$ ,  $\hat{B}_{\text{PR}} = W_{\text{PR}}^* B_{\text{PR}}$ , and  $\hat{C}_{\text{PR}} = L_w^T P_w^{-1}$ ) satisfies the projected Riccati equations with  $\hat{Q}_{\text{PR}} = P_w^{-1} > 0$

$$\hat{A}_{\text{PR}}^* \hat{Q}_{\text{PR}} + \hat{Q}_{\text{PR}} \hat{A}_{\text{PR}} + \hat{C}_{\text{PR}}^* \hat{C}_{\text{PR}} + \hat{Q}_{\text{PR}} \hat{B}_{\text{PR}} \hat{B}_{\text{PR}}^* \hat{Q}_{\text{PR}} = 0. \quad (54)$$

Since

$$\begin{aligned}\hat{A} &= S_w - L_w L_w^T P_w^{-1} + \hat{B}_{\text{PR}} L_w^T P_w^{-1}, \\ \hat{B} &= \hat{B}_{\text{PR}} R_{\text{PR}}^{\frac{1}{2}}, \quad \hat{C} = R_{\text{PR}}^{\frac{1}{2}} L_w^T P_w^{-1},\end{aligned}\tag{55}$$

the Riccati equation (54) can be rewritten as

$$\hat{A}^* \hat{Q}_{\text{PR}} + \hat{Q}_{\text{PR}} \hat{A} + (\hat{C} - \hat{B}^* \hat{Q}_{\text{PR}})^* R_{\text{PR}}^{-1} (\hat{C} - \hat{B}^* \hat{Q}_{\text{PR}}) = 0.\tag{56}$$

The RADI-based approximation of  $Q_{\text{PR}}$  is then given by  $W_{\text{PR}} P_w^{-1} W_{\text{PR}}^*$ .

**Theorem 2.4.** *Let  $G(s)$  be a positive-real transfer function. Define  $\tilde{L}_w^* = R_{\text{PR}}^{-\frac{1}{2}} (L_w^T - \hat{B}_{\text{PR}}^*) = \begin{bmatrix} l_{w,1}^* & \cdots & l_{w,q}^* \end{bmatrix}$  and  $T_w = \text{blkdiag}(l_{w,1}^*, \dots, l_{w,q}^*)$ . Assume that:*

1. *The interpolation points  $(\mu_1, \dots, \mu_w)$  are located in the right half of the  $s$ -plane.*
2. *The pair  $(S_w, \tilde{L}_w)$  is controllable.*
3. *The matrix  $T_w$  is invertible.*
4. *The realization  $(\hat{A}, \hat{B}, \hat{C})$  defined in (55) is minimal.*

*Then the following statements hold:*

1. *The projection matrix  $W_{\text{PR}}$  satisfies  $W_{\text{PR}} = \hat{W} T_w$ , where  $\hat{W}$  is as in (2).*
2. *The ROM  $\hat{G}(s) = \hat{C}(sI - \hat{A})^{-1} \hat{B} + D$  interpolates  $G(s)$  at  $(\mu_1, \dots, \mu_w)$ .*
3. *The ROM  $\hat{G}(s)$  is positive-real.*

*Proof.* The proof is similar to the proof of Theorem 2.3 and hence omitted for brevity.  $\square$

We now derive an expression for  $T_w$  when  $\hat{W}$  is used to enforce interpolation conditions instead of  $W_{\text{PR}}$ . Since  $W_{\text{PR}}$  and  $\hat{W}$  enforce identical interpolation

conditions, the following holds:

$$\begin{aligned}
\hat{B}_{\text{PR}} &= W_{\text{PR}}^* B_{\text{PR}} = \begin{bmatrix} G_{\text{PR}}(\mu_1) \\ \vdots \\ G_{\text{PR}}(\mu_w) \end{bmatrix} = \begin{bmatrix} \hat{G}_{\text{PR}}(\mu_1) \\ \vdots \\ \hat{G}_{\text{PR}}(\mu_w) \end{bmatrix} \\
&= \begin{bmatrix} R_{\text{PR}}^{-\frac{1}{2}} \zeta(\mu_1 I - S_w + L_w \zeta + \hat{W}^* B R_{\text{PR}}^{-1} \zeta)^{-1} \\ \vdots \\ R_{\text{PR}}^{-\frac{1}{2}} \zeta(\mu_w I - S_w + L_w \zeta + \hat{W}^* B R_{\text{PR}}^{-1} \zeta)^{-1} \end{bmatrix} \hat{W}^* B_{\text{PR}}, \\
&= T_w^* \hat{W}^* B R_{\text{PR}}^{-\frac{1}{2}},
\end{aligned}$$

where  $\hat{G}(s) = \zeta(sI - S_w + L_w \zeta)^{-1} \hat{W}^* B + D$  is an interpolant of  $G(s)$ . Such an interpolant can be generated by O-PORK, which guarantees stability, and  $T_w$  can be constructed from this interpolant by solving the Sylvester equation:

$$(S_w - L_w \zeta - \hat{W}^* B R_{\text{PR}}^{-1} \zeta)^* T_w - T_w S_w^* + \zeta^* R_{\text{PR}}^{-\frac{1}{2}} L_w^T = 0.$$

An immediate consequence is that positive-realness can be enforced non-intrusively on the ROM produced by O-PORK, using only samples of  $G(s)$  at  $\mu_i$  and  $G(\infty)$ . This is implemented in Algorithm 3, named ‘‘Data-driven Positive-real Interpolation ( $W$ -type) (DD-PRI- $W$ )’’. The resulting ROM is simply a different state-space realization of the ROM defined in (55).

Similar to the ADI-based non-intrusive implementation of BT, the RADI-based non-intrusive implementation of PR-BT can be directly obtained using the results of Theorems 2.3 and 2.4. The pseudo-code for this implementation, named ‘‘Data-driven PR-BT (DD-PR-BT)’’, is provided in Algorithm 4.

### 2.3. RADI-based Non-intrusive Implementation of BR-BT

By noting that  $D^T(I - DD^T)^{-1} = (I - D^T D)^{-1} D^T$ , define the following matrices:  $R_p = I - DD^T$ ,  $R_q = I - D^T D$ ,  $R_b = I + D^T R_p^{-1} D$ , and  $R_c = I + DR_q^{-1} D^T$ . Further, define the transfer functions

$$\begin{aligned}
G_{\text{BR}}^{\text{P}}(s) &= C_{\text{BR}}^{\text{P}}(sI - A_{\text{BR}})^{-1} B_{\text{BR}}^{\text{P}}, \\
G_{\text{BR}}^{\text{Q}}(s) &= C_{\text{BR}}^{\text{Q}}(sI - A_{\text{BR}})^{-1} B_{\text{BR}}^{\text{Q}},
\end{aligned}$$

---

**Algorithm 3** DD-PRI-W
 

---

**Input:** Interpolation points:  $(\mu_1, \dots, \mu_w)$ ; Data:  $(H(\mu_1), \dots, H(\mu_w))$  and  $G(\infty)$ .

**Output:** ROM:  $(\hat{A}, \hat{B}, \hat{C}, D)$

1: Compute  $\hat{B} = \hat{W}^* B$  from the samples  $H(\mu_i)$  via (5).

2: Set  $D = G(\infty)$  and  $R_{\text{PR}} = D + D^T$ .

3: Set  $S_w$  and  $L_w$  as in (6).

4: Compute  $P_w$  by solving the Lyapunov equations (10).

5: Compute  $T_w$  by solving the following Sylvester equation:

$$(S_w - L_w L_w^T P_w^{-1} - \hat{B} R_{\text{PR}}^{-1} L_w^T P_w^{-1})^* T_w - T_w S_w^* + P_w^{-1} L_w R_{\text{PR}}^{-\frac{1}{2}} L_w^T = 0.$$

6: Set  $\hat{B}_{\text{PR}} = T_w^* \hat{B} R_{\text{PR}}^{-\frac{1}{2}}$ .

7: Update  $P_w$  by solving the Lyapunov equations (53).

8: Set  $\hat{C} = R_{\text{PR}}^{\frac{1}{2}} L_w^T P_w^{-1} T_w^*$  and  $\hat{A} = S_w - L_w \hat{C}$ .

---

where

$$\begin{aligned} A_{\text{BR}} &= A + B D^T R_p^{-1} C = A + B R_q^{-1} D^T C, \\ B_{\text{BR}}^{\text{P}} &= B R_b^{\frac{1}{2}}, \quad C_{\text{BR}}^{\text{P}} = R_p^{-\frac{1}{2}} C, \\ B_{\text{BR}}^{\text{Q}} &= B R_q^{-\frac{1}{2}}, \quad C_{\text{BR}}^{\text{Q}} = R_c^{\frac{1}{2}} C. \end{aligned}$$

Next, define the ROMs

$$\begin{aligned} \hat{G}_{\text{BR}}^{\text{P}}(s) &= \hat{C}_{\text{BR}}^{\text{P}} (sI - \hat{A}_{\text{BR}})^{-1} \hat{B}_{\text{BR}}^{\text{P}}, \\ \hat{G}_{\text{BR}}^{\text{Q}}(s) &= \hat{C}_{\text{BR}}^{\text{Q}} (sI - \hat{A}_{\text{BR}})^{-1} \hat{B}_{\text{BR}}^{\text{Q}}, \end{aligned}$$

obtained as

$$\begin{aligned} \hat{A}_{\text{BR}} &= W_{\text{BR}}^* A_{\text{BR}} V_{\text{BR}} = \hat{A} + \hat{B} D^T R_p^{-1} \hat{C} = \hat{A} + \hat{B} R_q^{-1} D^T \hat{C}, \\ \hat{B}_{\text{BR}}^{\text{P}} &= W_{\text{BR}}^* B_{\text{BR}}^{\text{P}} = \hat{B} R_b^{\frac{1}{2}}, \quad \hat{C}_{\text{BR}}^{\text{P}} = C_{\text{BR}}^{\text{P}} V_{\text{BR}} = R_p^{-\frac{1}{2}} \hat{C}, \\ \hat{B}_{\text{BR}}^{\text{Q}} &= W_{\text{BR}}^* B_{\text{BR}}^{\text{Q}} = \hat{B} R_q^{-\frac{1}{2}}, \quad \hat{C}_{\text{BR}}^{\text{Q}} = C_{\text{BR}}^{\text{Q}} V_{\text{BR}} = R_c^{\frac{1}{2}} \hat{C}, \end{aligned}$$

where  $W_{\text{BR}}^* V_{\text{BR}} = I$ .

---

**Algorithm 4** DD-PR-BT

RADI shifts for approximating  $P_{\text{PR}}$ :  $(-\sigma_1, \dots, -\sigma_v)$ ; RADI shifts for approximating  $Q_{\text{PR}}$ :  $(-\mu_1, \dots, -\mu_w)$ ; Data:  $(H(\sigma_1), \dots, H(\sigma_v), H(\mu_1), \dots, H(\mu_w), G(\infty))$  and  $H'(\sigma_i)$  for  $\sigma_i = \mu_j$ ; Reduced order:  $r$ .

**Output:** ROM:  $(\hat{A}, \hat{B}, \hat{C}, D)$

- 1: Compute the Loewner quadruplet  $(\hat{W}^* \hat{V}, \hat{W}^* A \hat{V}, \hat{W}^* B, C \hat{V})$  from the samples  $H(\sigma_i)$  and  $H(\mu_i)$  via (5).
  - 2: Set  $D = G(\infty)$  and  $R_{\text{PR}} = D + D^T$ .
  - 3: Set  $S_v, L_v, S_w, L_w$  as in (6).
  - 4: Compute  $Q_v$  and  $P_w$  by solving the Lyapunov equations (9) and (10).
  - 5: Compute  $T_v$  and  $T_w$  by solving the following Sylvester equations:
 
$$(S_v - Q_v^{-1} L_v^T L_v - Q_v^{-1} L_v^T R_{\text{PR}}^{-1} C \hat{V}) T_v - T_v S_v + Q_v^{-1} L_v^T R_{\text{PR}}^{-\frac{1}{2}} L_v = 0,$$

$$(S_w - L_w L_w^T P_w^{-1} - \hat{W}^* B R_{\text{PR}}^{-1} L_w^T P_w^{-1})^* T_w - T_w S_w^* + P_w^{-1} L_w R_{\text{PR}}^{-\frac{1}{2}} L_w^T = 0.$$
  - 6: Set  $\hat{C}_{\text{PR}} = R_{\text{PR}}^{-\frac{1}{2}} C \hat{V} T_v$  and  $\hat{B}_{\text{PR}} = T_w^* \hat{W}^* B R_{\text{PR}}^{-\frac{1}{2}}$ .
  - 7: Update  $Q_v$  and  $P_w$  by solving the Lyapunov equations (42) and (53).
  - 8: Decompose  $Q_v^{-1}$  and  $P_w^{-1}$  as  $Q_v^{-1} = \hat{L}_p \hat{L}_p^*$  and  $P_w^{-1} = \hat{L}_q \hat{L}_q^*$ .
  - 9: Compute the following SVD:
 
$$\hat{L}_q^* T_w^* (\hat{W}^* \hat{V}) T_v \hat{L}_p = \begin{bmatrix} \tilde{U}_1 & \tilde{U}_2 \end{bmatrix} \begin{bmatrix} \tilde{\Sigma}_r & 0 \\ 0 & \tilde{\Sigma}_{n-r} \end{bmatrix} \begin{bmatrix} \tilde{V}_1^* \\ \tilde{V}_2^* \end{bmatrix}.$$
  - 10: Set  $W_r = T_w \hat{L}_q \tilde{U}_1 \tilde{\Sigma}_r^{-1/2}$  and  $V_r = T_v \hat{L}_p \tilde{V}_1 \tilde{\Sigma}_r^{-1/2}$ .
  - 11: Compute  $\hat{A}$ ,  $\hat{B}$ , and  $\hat{C}$  from (30).
-

The Riccati equations (22) and (23) can be rewritten as follows:

$$A_{\text{BR}}P_{\text{BR}} + P_{\text{BR}}A_{\text{BR}}^T + B_{\text{BR}}^{\text{P}}(B_{\text{BR}}^{\text{P}})^* + P_{\text{BR}}(C_{\text{BR}}^{\text{P}})^*C_{\text{BR}}^{\text{P}}P_{\text{BR}} = 0, \quad (57)$$

$$A_{\text{BR}}^TQ_{\text{BR}} + Q_{\text{BR}}A_{\text{BR}} + (C_{\text{BR}}^{\text{Q}})^*C_{\text{BR}}^{\text{Q}} + Q_{\text{BR}}B_{\text{BR}}^{\text{Q}}(B_{\text{BR}}^{\text{Q}})^*Q_{\text{BR}} = 0. \quad (58)$$

By applying Theorem 2.1, the RADI-based approximation of  $P_{\text{BR}}$  can be obtained as follows. The projection matrix

$$V_{\text{BR}} = \left[ (\sigma_1 I - A_{\text{BR}})^{-1} B_{\text{BR}}^{\text{P}} \quad \cdots \quad (\sigma_v I - A_{\text{BR}})^{-1} B_{\text{BR}}^{\text{P}} \right] \quad (59)$$

solves the following Sylvester equation:

$$A_{\text{BR}}V_{\text{BR}} - V_{\text{BR}}S_v + B_{\text{BR}}^{\text{P}}L_v = 0. \quad (60)$$

Then,  $\hat{C}_{\text{BR}}^{\text{P}} = C_{\text{BR}}^{\text{P}}V_{\text{BR}}$  can be computed as follows:

$$\hat{C}_{\text{BR}}^{\text{P}} = \left[ G_{\text{BR}}^{\text{P}}(\sigma_1) \quad \cdots \quad G_{\text{BR}}^{\text{P}}(\sigma_v) \right]. \quad (61)$$

Thereafter,  $Q_v$  is computed by solving the Lyapunov equation:

$$-S_v^*Q_v - Q_vS_v + L_v^T L_v - (\hat{C}_{\text{BR}}^{\text{P}})^* \hat{C}_{\text{BR}}^{\text{P}} = 0. \quad (62)$$

According to Theorem 2.1, the ROM ( $\hat{A}_{\text{BR}} = S_v - \hat{B}_{\text{BR}}^{\text{P}}L_v$ ,  $\hat{B}_{\text{BR}}^{\text{P}} = Q_v^{-1}L_v^T$ ,  $\hat{C}_{\text{BR}}^{\text{P}} = C_{\text{BR}}^{\text{P}}V_{\text{BR}}$ ) solves the following projected Riccati equation with  $\hat{P}_{\text{BR}} = Q_v^{-1} > 0$ :

$$\hat{A}_{\text{BR}}\hat{P}_{\text{BR}} + \hat{P}_{\text{BR}}\hat{A}_{\text{BR}}^* + \hat{B}_{\text{BR}}^{\text{P}}(\hat{B}_{\text{BR}}^{\text{P}})^* + \hat{P}_{\text{BR}}(\hat{C}_{\text{BR}}^{\text{P}})^*\hat{C}_{\text{BR}}^{\text{P}}\hat{P}_{\text{BR}} = 0. \quad (63)$$

Since

$$\begin{aligned} \hat{A} &= S_v - Q_v^{-1}L_v^T L_v - \hat{B}D^T R_p^{-1}\hat{C}, \\ \hat{B} &= Q_v^{-1}L_v^T R_b^{-\frac{1}{2}}, \quad \hat{C} = R_p^{\frac{1}{2}}C_{\text{BR}}^{\text{P}}V_{\text{BR}}, \end{aligned} \quad (64)$$

the Riccati equation (63) can be rewritten as

$$\hat{A}P_{\text{BR}} + \hat{P}_{\text{BR}}\hat{A}^* + \hat{B}\hat{B}^* + (\hat{P}_{\text{BR}}\hat{C}^* + \hat{B}D^T)R_p^{-1}(\hat{P}_{\text{BR}}\hat{C}^* + \hat{B}D^T)^* = 0.$$

**Theorem 2.5.** *Let  $G(s)$  be a bounded-real transfer function. Define  $\tilde{L}_v = D^T R_p^{-\frac{1}{2}}\hat{C}_{\text{BR}}^{\text{P}} + R_b^{\frac{1}{2}}L_v = \begin{bmatrix} l_{v,1} & \cdots & l_{v,p} \end{bmatrix}$  and  $T_v = \text{blkdiag}(l_{v,1}, \dots, l_{v,p})$ . Assume that:*

1. The interpolation points  $(\sigma_1, \dots, \sigma_v)$  are located in the right half of the  $s$ -plane.
2. The pair  $(S_v, \tilde{L}_v)$  is observable.
3. The matrix  $T_v$  is invertible.
4. The realization  $(\hat{A}, \hat{B}, \hat{C})$  defined in (64) is minimal.

Then the following statements hold:

1. The projection matrix  $V_{BR}$  is equal to  $\hat{V}T_v$  where  $\hat{V}$  is as in (1).
2. The ROM  $\hat{G}(s) = \hat{C}(sI - \hat{A})^{-1}\hat{B} + D$  interpolates  $G(s)$  at  $(\sigma_1, \dots, \sigma_p)$ .
3. The ROM  $\hat{G}(s)$  is bounded-real.

*Proof.* The proofs of 1 and 2 are similar to Theorem 2.3; hence, they are omitted for brevity.

By defining  $K_{BR} = (\hat{P}_{BR}\hat{C}^* + \hat{B}D^T)R_p^{-\frac{1}{2}}$ , the following relations hold:

$$\begin{aligned}\hat{A}\hat{P}_{BR} + \hat{P}_{BR}\hat{A}^* &= -\hat{B}\hat{B}^* - K_{BR}K_{BR}^*, \\ \hat{P}_{BR}\hat{C}^* + \hat{B}D^T &= -K_{BR}R_p^{\frac{1}{2}}, \\ R_p^{\frac{1}{2}}(R_p^{\frac{1}{2}})^* &= I - DD^T.\end{aligned}$$

Since  $\hat{P}_{BR} > 0$ ,  $\hat{G}(s)$  satisfies the bounded-real lemma [14].  $\square$

We now derive an expression for  $T_v$  when  $\hat{V}$  is used to enforce interpolation conditions instead of  $V_{BR}$ . Since  $V_{BR}$  and  $\hat{V}$  enforce the same interpolation conditions, the following holds:

$$\begin{aligned}\hat{C}_{BR}^P &= C_{BR}^P V_{BR} = \begin{bmatrix} G_{BR}^P(\sigma_1) & \cdots & G_{BR}^P(\sigma_v) \end{bmatrix} = \begin{bmatrix} \hat{G}_{BR}^P(\sigma_1) & \cdots & \hat{G}_{BR}^P(\sigma_v) \end{bmatrix} \\ &= C_{BR}^P \hat{V} \left[ (\sigma_1 I - S_v + \zeta L_v - \zeta D^T R_p^{-1} C \hat{V})^{-1} \zeta R_b^{\frac{1}{2}} \cdots (\sigma_v I - S_v + \zeta L_v - \zeta D^T R_p^{-1} C \hat{V})^{-1} \zeta R_b^{\frac{1}{2}} \right] \\ &= C_{BR}^P \hat{V} T_v = R_p^{-\frac{1}{2}} C \hat{V} T_v,\end{aligned}$$

where  $\hat{G}(s) = C\hat{V}(sI - S_v + \xi L_v)^{-1}\xi + D$  is an interpolant of  $G(s)$ . Such an interpolant can be produced by I-PORK, which is guaranteed to be stable, and  $T_v$  can be constructed from this interpolant. Specifically,  $T_v$  is the solution to the following Sylvester equation:

$$(S_v - \zeta L_v + \zeta D^T R_p^{-1} C \hat{V})T_v - T_v S_v + \zeta R_b^{\frac{1}{2}} L_v = 0.$$

An immediate consequence of this observation is that bounded-realness can be enforced non-intrusively on the ROM produced by I-PORK using only samples of  $G(s)$  at  $\sigma_i$  and the sample  $G(\infty)$ . This is implemented in Algorithm 5, named “Data-driven Bounded-real Interpolation (V-type) (DD-BRI-V)”. The resulting ROM is simply a different state-space realization of the ROM defined in (64).

---

**Algorithm 5** DD-BRI-V

---

**Input:** Interpolation points:  $(\sigma_1, \dots, \sigma_v)$ ; Data:  $(H(\sigma_1), \dots, H(\sigma_v))$  and  $G(\infty)$ .

**Output:** ROM:  $(\hat{A}, \hat{B}, \hat{C}, D)$

- 1: Compute  $\hat{C} = C\hat{V}$  from the samples  $H(\sigma_i)$  via (5).
  - 2: Set  $D = G(\infty)$   $R_p = I - DD^T$ , and  $R_b = I + D^T R_p^{-1} D$ .
  - 3: Set  $S_v$  and  $L_v$  as in (6).
  - 4: Compute  $Q_v$  by solving the Lyapunov equation (9).
  - 5: Compute  $T_v$  by solving the following Sylvester equation:
 
$$(S_v - Q_v^{-1} L_v^T L_v + Q_v^{-1} L_v^T D^T R_p^{-1} C\hat{V})T_v - T_v S_v + Q_v^{-1} L_v^T R_b^{-\frac{1}{2}} L_v = 0.$$
  - 6: Set  $\hat{C}_{\text{BR}}^{\text{P}} = R_p^{-\frac{1}{2}} \hat{C} T_v$ .
  - 7: Update  $Q_v$  by solving the Lyapunov equations (62).
  - 8: Set  $\hat{B} = T_v Q_v^{-1} L_v^T R_b^{-\frac{1}{2}}$  and  $\hat{A} = S_v - \hat{B} L_v$ .
- 

As per Theorem 2.2, the RADI-based approximation of  $Q_{\text{BR}}$  can be obtained as follows. The projection matrix

$$W_{\text{BR}}^* = \begin{bmatrix} C_{\text{BR}}^{\text{Q}} (\mu_1 I - A_{\text{BR}})^{-1} \\ \vdots \\ C_{\text{BR}}^{\text{Q}} (\mu_w I - A_{\text{BR}})^{-1} \end{bmatrix} \quad (65)$$

solves the following Sylvester equation:

$$A_{\text{BR}}^T W_{\text{BR}} - W_{\text{BR}} S_w^* + (C_{\text{BR}}^{\text{Q}})^* L_w^T = 0. \quad (66)$$

Then,  $\hat{B}_{\text{BR}}^{\text{Q}} = W_{\text{BR}}^* B_{\text{BR}}^{\text{Q}}$  can be computed as:

$$\hat{B}_{\text{BR}}^{\text{Q}} = \begin{bmatrix} G_{\text{BR}}^{\text{Q}}(\mu_1) \\ \vdots \\ G_{\text{BR}}^{\text{Q}}(\mu_w) \end{bmatrix}. \quad (67)$$

Thereafter,  $P_w$  is computed by solving the Lyapunov equation:

$$-S_w P_w - P_w S_w^* + L_w L_w^T - \hat{B}_{\text{BR}}^{\text{Q}} (\hat{B}_{\text{BR}}^{\text{Q}})^* = 0. \quad (68)$$

According to Theorem 2.2, the ROM ( $\hat{A}_{\text{BR}} = S_w - L_w \hat{C}_{\text{BR}}^{\text{Q}}$ ,  $\hat{B}_{\text{BR}}^{\text{Q}} = W_{\text{BR}}^* B_{\text{BR}}^{\text{Q}}$ ,  $\hat{C}_{\text{BR}}^{\text{Q}} = L_w^T P_w^{-1}$ ) solves the following projected Riccati equation with  $\hat{Q}_{\text{BR}} = P_w^{-1} > 0$ :

$$\hat{A}_{\text{BR}}^* \hat{Q}_{\text{BR}} + \hat{Q}_{\text{BR}} \hat{A}_{\text{BR}} + (\hat{C}_{\text{BR}}^{\text{Q}})^* \hat{C}_{\text{BR}}^{\text{Q}} + \hat{Q}_{\text{BR}} \hat{B}_{\text{BR}}^{\text{Q}} (\hat{B}_{\text{BR}}^{\text{Q}})^* \hat{Q}_{\text{BR}} = 0. \quad (69)$$

Since

$$\begin{aligned} \hat{A} &= S_w - L_w L_w^T P_w^{-1} - \hat{B} R_q^{-1} D^T \hat{C}, \\ \hat{B} &= \hat{W}_{\text{BR}}^* B_{\text{BR}}^{\text{Q}} R_q^{\frac{1}{2}}, \quad \hat{C} = R_c^{-\frac{1}{2}} L_w^T P_w^{-1}, \end{aligned} \quad (70)$$

the Riccati equation (69) can be rewritten as:

$$\hat{A}^* \hat{Q}_{\text{BR}} + \hat{Q}_{\text{BR}} \hat{A} + \hat{C}^* \hat{C} + (\hat{B}^* \hat{Q}_{\text{BR}} + D^T \hat{C})^* R_q^{-1} (\hat{B}^* \hat{Q}_{\text{BR}} + D^T \hat{C}) = 0. \quad (71)$$

The RADI-based approximation of  $Q_{\text{BR}}$  is given by  $W_{\text{BR}} P_w^{-1} W_{\text{BR}}^*$ .

**Theorem 2.6.** *Let  $G(s)$  be a bounded-real transfer function. Define  $\tilde{L}_w^* = D^T R_p^{-\frac{1}{2}} \hat{B}_{\text{BR}}^{\text{Q}} + R_c^{\frac{1}{2}} L_w^T = \begin{bmatrix} l_{w,1}^* & \cdots & l_{w,q}^* \end{bmatrix}$  and  $T_w = \text{blkdiag}(l_{w,1}^*, \dots, l_{w,q}^*)$ . Assume that:*

1. *The interpolation points  $(\mu_1, \dots, \mu_w)$  are located in the right half of the  $s$ -plane.*
2. *The pair  $(S_w, \tilde{L}_w)$  is controllable.*
3. *The matrix  $T_w$  is invertible.*
4. *The realization  $(\hat{A}, \hat{B}, \hat{C})$  defined in (70) is minimal.*

*Then the following statements hold:*

1. The projection matrix  $W_{BR}$  is equal to  $\hat{W}T_w$  where  $\hat{W}$  is as in (2).
2. The ROM  $\hat{G}(s) = \hat{C}(sI - \hat{A})^{-1}\hat{B} + D$  interpolates  $G(s)$  at  $(\mu_1, \dots, \mu_q)$ .
3. The ROM  $\hat{G}(s)$  is bounded-real.

*Proof.* The proof is similar to that of Theorem 2.5 and hence omitted for brevity.  $\square$

We now derive an expression for  $T_w$  when  $\hat{W}$  is used to enforce interpolation conditions instead of  $W_{BR}$ . Since  $W_{BR}$  and  $\hat{W}$  enforce identical interpolation conditions, the following holds:

$$\begin{aligned} \hat{B}_{BR}^Q &= W_{BR}^* B_{BR}^Q = \begin{bmatrix} G_{BR}^Q(\mu_1) \\ \vdots \\ G_{BR}^Q(\mu_w) \end{bmatrix} = \begin{bmatrix} \hat{G}_{PR}^Q(\mu_1) \\ \vdots \\ \hat{G}_{PR}^Q(\mu_w) \end{bmatrix} \\ &= \begin{bmatrix} R_c^{\frac{1}{2}} \zeta(\mu_1 I - S_w + L_w \zeta - \hat{W}^* B R_q^{-1} D^T \zeta)^{-1} \\ \vdots \\ R_c^{\frac{1}{2}} \zeta(\mu_w I - S_w + L_w \zeta - \hat{W}^* B R_q^{-1} D^T \zeta)^{-1} \end{bmatrix} \hat{W}^* B_{BR}^Q, \\ &= T_w^* \hat{W}^* B R_q^{-\frac{1}{2}}, \end{aligned}$$

where  $\hat{G}(s) = \zeta(sI - S_w + L_w \zeta)^{-1} \hat{W}^* B + D$  is an interpolant of  $G(s)$ . This interpolant can be produced by O-PORK, which is guaranteed to be stable, and  $T_w$  can be constructed from it. Specifically,  $T_w$  is obtained by solving the Sylvester equation:

$$(S_w - L_w \zeta + \hat{W}^* B R_q^{-1} D^T \zeta)^* T_w - T_w S_w^* + \zeta^* R_c^{\frac{1}{2}} L_w^T = 0. \quad (72)$$

An immediate consequence is that bounded-realness can be enforced non-intrusively on the ROM produced by O-PORK, using only samples of  $G(s)$  at  $\mu_i$  and  $G(\infty)$ . This approach is implemented in Algorithm 6, named ‘‘Data-driven Bounded-real Interpolation ( $W$ -type) (DD-BRI- $W$ )’’. The resulting ROM represents a different state-space realization of the ROM defined in (70).

Similar to the ADI-based non-intrusive implementation of BT, the RADI-based non-intrusive implementation of BR-BT can be directly obtained using the results of Theorems 2.5 and 2.6. The pseudo-code for this implementation, named ‘‘Data-driven BR-BT (DD-BR-BT)’’, is provided in Algorithm 7.

---

**Algorithm 6** DD-BRI-W

---

**Input:** Interpolation points:  $(\mu_1, \dots, \mu_w)$ ; Data:  $(H(\mu_1), \dots, H(\mu_w))$  and  $G(\infty)$ .

**Output:** ROM:  $(\hat{A}, \hat{B}, \hat{C}, D)$

- 1: Compute  $\hat{B} = \hat{W}^* B$  from the samples  $H(\mu_i)$  via (5).
  - 2: Set  $D = G(\infty)$ ,  $R_q = I - D^T D$ , and  $R_c = I + D R_q^{-1} D^T$ .
  - 3: Set  $S_w$  and  $L_w$  as in (6).
  - 4: Compute  $P_w$  by solving the Lyapunov equations (10).
  - 5: Compute  $T_w$  by solving the following Sylvester equation:  
$$(S_w - L_w L_w^T P_w^{-1} + \hat{W}^* B R_q^{-1} D^T L_w^T P_w^{-1})^* T_w - T_w S_w^* + P_w^{-1} L_w R_c^{\frac{1}{2}} L_w^T = 0.$$
  - 6: Set  $\hat{B}_{\text{PR}} = T_w^* \hat{B} R_q^{-\frac{1}{2}}$ .
  - 7: Update  $P_w$  by solving the Lyapunov equations (68).
  - 8: Set  $\hat{C} = R_c^{-\frac{1}{2}} L_w^T P_w^{-1} T_w^*$  and  $\hat{A} = S_w - L_w \hat{C}$ .
- 

#### 2.4. ADI-based Non-intrusive Implementation of SW-BT

Let us define the transfer function

$$G_{\text{SW}}(s) = C_{\text{SW}}(sI - A_{\text{SW}})^{-1} B,$$

where  $A_{\text{SW}} = A - B C_{\text{SW}}$  and  $C_{\text{SW}} = D^{-1} C$ . Next, define the ROM  $\hat{G}_{\text{SW}}(s)$

$$\hat{G}_{\text{SW}}(s) = \hat{C}_{\text{SW}}(sI - \hat{A}_{\text{SW}})^{-1} \hat{B},$$

obtained as

$$\begin{aligned} \hat{A}_{\text{SW}} &= W_{\text{SW}}^* A_{\text{SW}} \hat{V} = \hat{A} - \hat{B} D^{-1} \hat{C}, \\ \hat{B} &= W_{\text{SW}}^* B, \quad \hat{C}_{\text{SW}} = C_{\text{SW}} V_{\text{SW}} = D^{-1} \hat{C}, \end{aligned}$$

where  $W_{\text{SW}}^* V_{\text{SW}} = I$ .

The Lyapunov equation (24) can be rewritten as:

$$A_{\text{SW}}^T Q_{\text{SW}} + Q_{\text{SW}} A_{\text{SW}} + C_{\text{SW}}^T C_{\text{SW}} = 0. \quad (73)$$

The O-PORK-based approximation of  $Q_{\text{SW}}$  (equivalent to the ADI method) is computed as follows. First, solve the Sylvester equation for the projection

---

**Algorithm 7** DD-BR-BT

RADI shifts for approximating  $P_{\text{BR}}$ :  $(-\sigma_1, \dots, -\sigma_v)$ ; RADI shifts for approximating  $Q_{\text{BR}}$ :  $(-\mu_1, \dots, -\mu_w)$ ; Data:  $(H(\sigma_1), \dots, H(\sigma_v), H(\mu_1), \dots, H(\mu_w), G(\infty))$  and  $H'(\sigma_i)$  for  $\sigma_i = \mu_j$ ; Reduced order:  $r$ .

**Output:** ROM:  $(\hat{A}, \hat{B}, \hat{C}, D)$

- 1: Compute the Loewner quadruplet  $(\hat{W}^* \hat{V}, \hat{W}^* A \hat{V}, \hat{W}^* B, C \hat{V})$  from the samples  $H(\sigma_i)$  and  $H(\mu_i)$  via (5).
  - 2: Set  $D = G(\infty)$ ,  $R_p = I - DD^T$ ,  $R_b = I + D^T R_p^{-1} D$ ,  $R_q = I - D^T D$ , and  $R_c = I + DR_q^{-1} D^T$ .
  - 3: Set  $S_v$ ,  $L_v$ ,  $S_w$ , and  $L_w$  as in (6).
  - 4: Compute  $Q_v$  and  $P_w$  by solving the Lyapunov equations (9) and (10).
  - 5: Compute  $T_v$  and  $T_w$  by solving the following Sylvester equations:
 
$$(S_v - Q_v^{-1} L_v^T L_v + Q_v^{-1} L_v^T D^T R_p^{-1} C \hat{V}) T_v - T_v S_v + Q_v^{-1} L_v^T R_b^{-\frac{1}{2}} L_v = 0,$$

$$(S_w - L_w L_w^T P_w^{-1} + \hat{W}^* B R_q^{-1} D^T L_w^T P_w^{-1})^* T_w - T_w S_w^* + P_w^{-1} L_w R_c^{-\frac{1}{2}} L_w^T = 0.$$
  - 6: Set  $\hat{C}_{\text{BR}}^{\text{P}} = R_p^{-\frac{1}{2}} C \hat{V} T_v$  and  $\hat{B}_{\text{BR}}^{\text{Q}} = T_w^* \hat{W}^* B R_q^{-\frac{1}{2}}$ .
  - 7: Update  $Q_v$  and  $P_w$  by solving the Lyapunov equations (62) and (68).
  - 8: Decompose  $Q_v^{-1}$  and  $P_w^{-1}$  as  $Q_v^{-1} = \hat{L}_p \hat{L}_p^*$  and  $P_w^{-1} = \hat{L}_q \hat{L}_q^*$ .
  - 9: Compute the following SVD:
 
$$\hat{L}_q^* T_w^* (\hat{W}^* \hat{V}) T_v \hat{L}_p = \begin{bmatrix} \tilde{U}_1 & \tilde{U}_2 \end{bmatrix} \begin{bmatrix} \tilde{\Sigma}_r & 0 \\ 0 & \tilde{\Sigma}_{n-r} \end{bmatrix} \begin{bmatrix} \tilde{V}_1^* \\ \tilde{V}_2^* \end{bmatrix}.$$
  - 10: Set  $W_r = T_w \hat{L}_q \tilde{U}_1 \tilde{\Sigma}_r^{-1/2}$  and  $V_r = T_v \hat{L}_p \tilde{V}_1 \tilde{\Sigma}_r^{-1/2}$ .
  - 11: Compute  $\hat{A}$ ,  $\hat{B}$ , and  $\hat{C}$  from (30).
-

matrix  $W_{\text{SW}}$ :

$$A_{\text{SW}}^T W_{\text{SW}} - W_{\text{SW}} S_w^* + C_{\text{SW}}^T L_w^T = 0. \quad (74)$$

Then, compute  $P_w$  by solving the Lyapunov equation (10). The ADI-based approximation of  $Q_{\text{SW}}$  is obtained as:  $Q_{\text{S}} \approx W_{\text{SW}} P_w^{-1} W_{\text{SW}}^*$ . The following ROM  $\hat{G}(s)$  can be recovered from the ROM  $\hat{G}_{\text{SW}}(s) = L_w^T P_w^{-1} (sI - S_w + L_w L_w^T P_w^{-1})^{-1} W_{\text{SW}}^* B$  produced by O-PORK:

$$\begin{aligned} \hat{A} &= S_w + L_w L_w^T P_w^{-1} + W_{\text{S}}^* B L_w^T P_w^{-1}, \\ \hat{B} &= W_{\text{SW}}^* B, \quad \hat{C} = D L_w^T P_w^{-1}. \end{aligned} \quad (75)$$

**Theorem 2.7.** *Let  $G(s)$  be a square stable minimum phase transfer function.*

*Define  $\tilde{L}_w^* = D^{-T} (L_w^T - \hat{B}^*) = [l_{w,1}^* \quad \cdots \quad l_{w,q}^*]$  and  $T_w = \text{blkdiag}(l_{w,1}^*, \dots, l_{w,q}^*)$ .*

*Assume that:*

1. *The interpolation points  $(\mu_1, \dots, \mu_w)$  are located in the right half of the  $s$ -plane.*
2. *The pair  $(S_w, \tilde{L}_w)$  is controllable.*
3. *The matrix  $T_w$  is invertible.*
4. *The realization  $(\hat{A}, \hat{B}, \hat{C})$  defined in (75) is minimal.*

*Then the following statements hold:*

1. *The projection matrix  $W_{\text{SW}}$  is equal to  $\hat{W} T_w$  where  $\hat{W}$  is as in (2).*
2. *The ROM  $\hat{G}(s) = \hat{C} (sI - \hat{A})^{-1} \hat{B} + D$  interpolates  $G(s)$  at  $(\mu_1, \dots, \mu_q)$ .*
3. *The ROM  $\hat{G}(s)$  is minimum phase.*

*Proof.* The proof of 1 and 2 is similar to that of Theorem 2.4 and hence omitted for brevity.

The zeros of  $\hat{G}(s)$ , i.e., the eigenvalues of  $\hat{A}_{\text{SW}} = \hat{A} - \hat{B} D^{-1} \hat{C}$ , are  $(-\mu_1^*, \dots, -\mu_w^*)$  in O-PORK. Since the interpolation points in O-PORK are in the right half of the  $s$ -plane,  $\hat{A}_{\text{SW}}$  is Hurwitz and  $\hat{G}(s)$  is minimum phase.  $\square$

We now derive an expression for  $T_w$  when  $\hat{W}$  is used for enforcing interpolation conditions instead of  $W_{\text{SW}}$ . Since  $W_{\text{SW}}$  and  $\hat{W}$  enforce the same interpolation conditions, the following holds:

$$\begin{aligned}\hat{B} &= W_{\text{SW}}^* B = \begin{bmatrix} G_{\text{SW}}(\mu_1) \\ \vdots \\ G_{\text{SW}}(\mu_w) \end{bmatrix} = \begin{bmatrix} \hat{G}_{\text{SW}}(\mu_1) \\ \vdots \\ \hat{G}_{\text{SW}}(\mu_w) \end{bmatrix} \\ &= \begin{bmatrix} D^{-1}\zeta(\mu_1 I - S_w + L_w \zeta + \hat{W}^* B D^{-1} \zeta)^{-1} \\ \vdots \\ D^{-1}\zeta(\mu_w I - S_w + L_w \zeta + \hat{W}^* B D^{-1} \zeta)^{-1} \end{bmatrix} \hat{W}^* B, \\ &= T_w^* \hat{W}^* B,\end{aligned}$$

where  $\hat{G}(s) = \zeta(sI - S_w + L_w \zeta)^{-1} \hat{W}^* B + D$  is the interpolant of  $G(s)$ . Such an interpolant can be produced by O-PORK, which is guaranteed to be stable, and  $T_w$  can be constructed from this interpolant.  $T_w$  can be computed by solving the following Sylvester equation:

$$(S_w - L_w \zeta - \hat{W}^* B D^{-1} \zeta)^* T_w - T_w S_w^* + \zeta^* D^{-T} L_w^T = 0.$$

An immediate consequence of this observation is that the minimum-phase property can be enforced on the ROM nonintrusively produced by O-PORK using only samples of  $G(s)$  at  $\mu_i$  and the sample  $G(\infty)$ . This is implemented in Algorithm 8, named ‘‘Data-driven Minimum-phase Interpolation (DD-MPI)’’. The resulting ROM is simply a different state-space realization of the ROM defined in (75).

Similar to the ADI-based nonintrusive implementation of BT, the ADI-based nonintrusive implementation of SW-BT can be derived directly using the results of Theorem 2.7. The pseudo-code for this implementation, named ‘‘Data-driven SW-BT (DD-SW-BT)’’, is provided in Algorithm 9.

### 2.5. ADI/RADI-based Non-intrusive Implementation of BST

Let us define the transfer function

$$G_{\text{S}}(s) = C_{\text{S}}(sI - A_{\text{S}})^{-1} B_{\text{S}},$$

---

**Algorithm 8** DD-MPI

---

**Input:** Interpolation points:  $(\mu_1, \dots, \mu_w)$ ; Data:  $(H(\mu_1), \dots, H(\mu_w))$  and  $G(\infty)$ .

**Output:** ROM:  $(\hat{A}, \hat{B}, \hat{C}, D)$

- 1: Compute  $\hat{B} = \hat{W}^* B$  from the samples  $H(\mu_i)$  via (5) and set  $D = G(\infty)$ .
  - 2: Set  $S_w$  and  $L_w$  as in (6).
  - 3: Compute  $P_w$  by solving the Lyapunov equations (10).
  - 4: Compute  $T_w$  by solving the following Sylvester equation:  
$$(S_w - L_w L_w^T P_w^{-1} - \hat{B} D^{-1} L_w^T P_w^{-1})^* T_w - T_w S_w^* + P_w^{-1} L_w D^{-T} L_w^T = 0.$$
  - 5: Set  $\hat{C} = D L_w^T P_w^{-1} T_w^*$  and  $\hat{A} = S_w - L_w \hat{C}$ .
- 

---

**Algorithm 9** DD-SW-BT

---

ADI shifts for approximating  $P$ :  $(-\sigma_1, \dots, -\sigma_v)$ ; ADI shifts for approximating  $Q_{\text{sw}}$ :  $(-\mu_1, \dots, -\mu_w)$ ; Data:  $(H(\sigma_1), \dots, H(\sigma_v), H(\mu_1), \dots, H(\mu_w), G(\infty))$  and  $H'(\sigma_i)$  for  $\sigma_i = \mu_j$ ; Reduced order:  $r$ .

**Output:** ROM:  $(\hat{A}, \hat{B}, \hat{C}, D)$

- 1: Compute the Loewner quadruplet  $(\hat{W}^* \hat{V}, \hat{W}^* A \hat{V}, \hat{W}^* B, C \hat{V})$  from the samples  $H(\sigma_i)$  and  $H(\mu_i)$  via (5) and set  $D = G(\infty)$ .
  - 2: Set  $S_v, L_v, S_w$ , and  $L_w$  as in (6).
  - 3: Compute  $Q_v$  and  $P_w$  by solving the Lyapunov equations (9) and (10).
  - 4: Compute  $T_w$  by solving the following Sylvester equation:  
$$(S_w - L_w L_w^T P_w^{-1} - \hat{B} D^{-1} L_w^T P_w^{-1})^* T_w - T_w S_w^* + P_w^{-1} L_w D^{-T} L_w^T = 0.$$
  - 5: Decompose  $Q_v^{-1}$  and  $P_w^{-1}$  as  $Q_v^{-1} = \hat{L}_p \hat{L}_p^*$  and  $P_w^{-1} = \hat{L}_q \hat{L}_q^*$ .
  - 6: Compute the following SVD:  
$$\hat{L}_q^* T_w^* (\hat{W}^* \hat{V}) \hat{L}_p = \begin{bmatrix} \tilde{U}_1 & \tilde{U}_2 \end{bmatrix} \begin{bmatrix} \tilde{\Sigma}_r & 0 \\ 0 & \tilde{\Sigma}_{n-r} \end{bmatrix} \begin{bmatrix} \tilde{V}_1^* \\ \tilde{V}_2^* \end{bmatrix}.$$
  - 7: Set  $W_r = T_w \hat{L}_q \tilde{U}_1 \tilde{\Sigma}_r^{-1/2}$  and  $V_r = \hat{L}_p \tilde{V}_1 \tilde{\Sigma}_r^{-1/2}$ .
  - 8: Compute  $\hat{A}$ ,  $\hat{B}$ , and  $\hat{C}$  from (30).
-

where

$$\begin{aligned} A_S &= A - B_S C_S, & B_S &= (P C^T + B D^T) R_S^{-\frac{1}{2}}, \\ C_S &= R_S^{-\frac{1}{2}} C, & R_S &= D D^T. \end{aligned}$$

The Riccati equation (25) can be rewritten as follows:

$$A_S^T Q_S + Q_S A_S + C_S^T C_S + Q_S B_S B_S^T Q_S = 0. \quad (76)$$

Unlike the Riccati equations considered up until now, the RADI-based approximation of this Riccati equation is a bit more involved. We first need to replace  $B_S$  with its approximation. Let us replace  $P$  in  $B_S$  with  $\hat{V} Q_v^{-1} \hat{V}^*$ , which is an ADI-based approximation of  $P$  obtained via I-PORK. Then,  $B_S \approx \tilde{B}_S = (\hat{V} Q_v^{-1} \hat{V}^* C^T + B D^T) R_S^{-\frac{1}{2}}$  and  $A_S \approx \tilde{A}_S = A - \tilde{B}_S C_S$ . Thereafter, we proceed with the RADI-based approximation of the following Riccati equation:

$$\tilde{A}_S^* \tilde{Q}_S + \tilde{Q}_S \tilde{A}_S + C_S^* C_S + \tilde{Q}_S \tilde{B}_S \tilde{B}_S^* \tilde{Q}_S = 0. \quad (77)$$

The RADI-based approximation of  $\tilde{Q}_S$  can be obtained using Theorem 2.2 as follows. The projection matrix  $W_S$  is computed by solving the following Sylvester equation:

$$\tilde{A}_S^* W_S - W_S S_w^* + C_S^T L_w^T = 0. \quad (78)$$

The matrix  $P_w$  is computed by solving the following Sylvester equation:

$$-S_w P_w - P_w S_w^* + L_w L_w^T - \hat{B}_S \hat{B}_S^* = 0, \quad (79)$$

where  $\hat{B}_S = W_S^* \tilde{B}_S$ .

Once again, it can be shown that  $W_S$  and  $\hat{W}$  in (2) enforce the same interpolation conditions and  $W_S = \hat{W} T_w$ , where  $T_w$  is invertible. The proof is similar and hence omitted here for brevity.

Let us define the ROM

$$\hat{G}_S(s) = \hat{C}_S (sI - \hat{A}_S)^{-1} \hat{B}_S,$$

obtained as

$$\hat{A}_S = W_S^* \tilde{A}_S V_S, \quad \hat{B}_S = W_S^* \tilde{B}_S, \quad \hat{C}_S = C_S V_S,$$

where  $W_S^* V_S = I$ .

We now derive an expression for  $T_w$  when  $\hat{W}$  is used for enforcing interpolation conditions instead of  $W_S$ . Since  $W_S$  and  $\hat{W}$  enforce the same interpolation conditions, the following holds:

$$\begin{aligned} \hat{B}_S &= W_S^* \tilde{B}_S = \begin{bmatrix} G_S(\mu_1) \\ \vdots \\ G_S(\mu_w) \end{bmatrix} = \begin{bmatrix} \hat{G}_S(\mu_1) \\ \vdots \\ \hat{G}_S(\mu_w) \end{bmatrix} \\ &= \begin{bmatrix} R_S^{-\frac{1}{2}} \zeta (\mu_1 I - S_w + L_w \zeta + (\hat{W}^* \hat{V} Q_v^{-1} \hat{V}^* C^T + \hat{W}^* B D^T) R_S^{-1} \zeta)^{-1} \\ \vdots \\ R_S^{-\frac{1}{2}} \zeta (\mu_w I - S_w + L_w \zeta + (\hat{W}^* \hat{V} Q_v^{-1} \hat{V}^* C^T + \hat{W}^* B D^T) R_S^{-1} \zeta)^{-1} \end{bmatrix} \hat{W}^* B_X, \\ &= T_w^* \hat{W}^* B_S, \\ &= T_w^* ((\hat{W}^* \hat{V}) Q_v^{-1} (C \hat{V})^* + (\hat{W}^* B) D^T) R_S^{-\frac{1}{2}}, \end{aligned}$$

where  $\hat{G}(s) = \zeta (sI - S_w + L_w \zeta)^{-1} \hat{W}^* B + D$  is the interpolant of  $G(s)$ . Such an interpolant can be produced by O-PORK, which is guaranteed to be stable.  $T_w$  can be constructed from this interpolant by solving the following Sylvester equation:

$$(S_w - L_w \zeta - [(\hat{W}^* \hat{V}) Q_v^{-1} (C \hat{V})^* + (\hat{W}^* B) D^T] R_S^{-1} \zeta)^* T_w - T_w S_w^* + \zeta^* R_S^{-\frac{1}{2}} L_w^T = 0.$$

Similar to the ADI-based nonintrusive implementation of BT, the ADI- and RADI-based nonintrusive implementation of BST can be obtained readily. The pseudo-code for this implementation, named ‘‘Data-driven BST (DD-BST)’’, is provided in Algorithm 10.

### 3. Practical Considerations in Implementation

The theoretical foundations of the ADI [19] and RADI [4] methods are well established. Their performance in approximating Lyapunov and Riccati equations is also well documented. However, the implementation presented in this

---

**Algorithm 10** DD-BST

---

ADI shifts for approximating  $P$ :  $(-\sigma_1, \dots, -\sigma_v)$ ; RADI shifts for approximating  $Q_S$ :  $(-\mu_1, \dots, -\mu_w)$ ; Data:  $(H(\sigma_1), \dots, H(\sigma_v), H(\mu_1), \dots, H(\mu_w), G(\infty))$  and  $H'(\sigma_i)$  for  $\sigma_i = \mu_j$ ; Reduced order:  $r$ .

**Output:** ROM:  $(\hat{A}, \hat{B}, \hat{C}, D)$

- 1: Compute the Loewner quadruplet  $(\hat{W}^* \hat{V}, \hat{W}^* A \hat{V}, \hat{W}^* B, C \hat{V})$  from the samples  $H(\sigma_i)$  and  $H(\mu_i)$  via (5).
- 2: Set  $D = G(\infty)$  and  $R_S = DD^T$ .
- 3: Set  $S_v, L_v, S_w,$  and  $L_w$  as in (6).
- 4: Compute  $Q_v$  and  $P_w$  by solving the Lyapunov equations (9) and (10).

- 5: Compute  $T_w$  by solving the following Sylvester equation:

$$(S_w - L_w L_w^T P_w^{-1} - [(\hat{W}^* \hat{V}) Q_v^{-1} (C \hat{V})^* + (\hat{W}^* B) D^T] R_S^{-1} L_w^T P_w^{-1})^* T_w - T_w S_w^* + P_w^{-1} L_w R_S^{-\frac{1}{2}} L_w^T = 0.$$

- 6: Set  $\hat{B}_S = T_w^* ((\hat{W}^* \hat{V}) Q_v^{-1} (C \hat{V})^* + (\hat{W}^* B) D^T) R_S^{-\frac{1}{2}}$ .

- 7: Update  $P_w$  by solving the Sylvester equation (79).

- 8: Decompose  $Q_v^{-1}$  and  $P_w^{-1}$  as  $Q_v^{-1} = \hat{L}_p \hat{L}_p^*$  and  $P_w^{-1} = \hat{L}_q \hat{L}_q^*$ .

- 9: Compute the following SVD:

$$\hat{L}_q^* T_w^* (\hat{W}^* \hat{V}) \hat{L}_p = \begin{bmatrix} \tilde{U}_1 & \tilde{U}_2 \end{bmatrix} \begin{bmatrix} \tilde{\Sigma}_r & 0 \\ 0 & \tilde{\Sigma}_{n-r} \end{bmatrix} \begin{bmatrix} \tilde{V}_1^* \\ \tilde{V}_2^* \end{bmatrix}.$$

- 10: Set  $W_r = T_w \hat{L}_q \tilde{U}_1 \tilde{\Sigma}_r^{-1/2}$  and  $V_r = \hat{L}_p \tilde{V}_1 \tilde{\Sigma}_r^{-1/2}$ .

- 11: Compute  $\hat{A}, \hat{B},$  and  $\hat{C}$  from (30).
-

paper involves inverses  $Q_v^{-1}$  and  $P_w^{-1}$ , which can cause numerical problems as the number of samples used for implementation increases. This is because the solution of Lyapunov equations is generally low-rank, enabling low-rank approximation via the low-rank ADI method [19] in the first place. Thus, as the number of samples used for implementation increases, the matrices  $Q_v$  and  $P_w$  start losing rank. Note that these matrices do not appear in the original algorithms. In data-driven modeling, one typically uses as many samples as available to ensure maximum accuracy. As discussed in [2], the inverses  $Q_v^{-1}$  and  $P_w^{-1}$  can be computed conveniently when the interpolation points are lightly damped, i.e.,

$$\sigma_i = \left( \frac{\zeta_{i,\sigma} |\omega_{i,\sigma}|}{\sqrt{1 - \zeta_{i,\sigma}^2}} \right) + j\omega_{i,\sigma} \quad \text{and} \quad \mu_i = \left( \frac{\zeta_{i,\mu} |\omega_{i,\mu}|}{\sqrt{1 - \zeta_{i,\mu}^2}} \right) + j\omega_{i,\mu}, \quad (80)$$

wherein  $\zeta_{i,\sigma} \ll 1$  and  $\zeta_{i,\mu} \ll 1$ . If we select the damping coefficients  $\zeta_{i,\sigma} \approx 0$  and  $\zeta_{i,\mu} \approx 0$ , this means we are sampling  $G(s)$  in close proximity to the  $j\omega$ -axis, which is also practically reasonable for capturing the frequency response of  $G(s)$ . When the interpolation points are lightly damped (i.e.,  $\zeta_{i,\sigma} \ll 1$  and  $\zeta_{i,\mu} \ll 1$ ),  $Q_v$ ,  $P_w$ ,  $Q_v^{-1}$ , and  $P_w^{-1}$  become diagonally dominant. If  $\zeta_{i,\sigma} \approx 0$  and  $\zeta_{i,\mu} \approx 0$ , the off-diagonal elements are nearly zero. For details, refer to [22]. Essentially, this means that each diagonal element of  $Q_v^{-1}$  and  $P_w^{-1}$  depends solely on its respective pair  $(\sigma_i, G(\sigma_i))$  or  $(\mu_i, G(\mu_i))$ , while the dependence on other samples or sampling points becomes negligible.

Assuming that the interpolation points are lightly damped, we can derive the expressions for the diagonal entries of  $Q_v^{-1}$  and  $P_w^{-1}$  as follows:

For DD-LQG-BT:

$$Q_v^{-1} \approx \text{blkdiag}(2\text{Real}(\sigma_1)[I_m + H^*(\sigma_1)H(\sigma_1)]^{-1}, \dots, 2\text{Real}(\sigma_v)[I_m + H^*(\sigma_v)H(\sigma_v)]^{-1}), \quad (81)$$

$$P_w^{-1} \approx \text{blkdiag}(2\text{Real}(\mu_1)[I_p + H(\mu_1)H^*(\mu_1)]^{-1}, \dots, 2\text{Real}(\mu_w)[I_p + H(\mu_w)H^*(\mu_w)]^{-1}). \quad (82)$$

For DD- $\mathcal{H}_\infty$ -BT:

$$Q_v^{-1} \approx \text{blkdiag}(2\text{Real}(\sigma_1)[I_m + (1 - \gamma^{-2})H^*(\sigma_1)H(\sigma_1)]^{-1}, \dots, \\ 2\text{Real}(\sigma_v)[I_m + (1 - \gamma^{-2})H^*(\sigma_v)H(\sigma_v)]^{-1}), \quad (83)$$

$$P_w^{-1} \approx \text{blkdiag}(2\text{Real}(\mu_1)[I_p + (1 - \gamma^{-2})H(\mu_1)H^*(\mu_1)]^{-1}, \dots, \\ 2\text{Real}(\mu_w)[I_p + (1 - \gamma^{-2})H(\mu_w)H^*(\mu_w)]^{-1}). \quad (84)$$

For DD-PR-BT:

$$Q_v^{-1} \approx \text{blkdiag}(2\text{Real}(\sigma_1)[I_m - t_{v,1}^* H^*(\sigma_1) R_{\text{PR}}^{-1} H(\sigma_1) t_{v,1}]^{-1}, \dots, \\ 2\text{Real}(\sigma_v)[I_m - t_{v,v}^* H^*(\sigma_v) R_{\text{PR}}^{-1} H(\sigma_v) t_{v,v}]^{-1}), \quad (85)$$

$$P_w^{-1} \approx \text{blkdiag}(2\text{Real}(\mu_1)[I_p - t_{w,1}^* H(\mu_1) R_{\text{PR}}^{-1} H^*(\mu_1) t_{w,1}]^{-1}, \dots, \\ 2\text{Real}(\mu_w)[I_p - t_{w,w}^* H(\mu_w) R_{\text{PR}}^{-1} H^*(\mu_w) t_{w,w}]^{-1}), \quad (86)$$

$$T_v \approx \text{blkdiag}(t_{v,1}, \dots, t_{v,v}), \quad (87)$$

$$T_w \approx \text{blkdiag}(t_{w,1}, \dots, t_{w,w}), \quad (88)$$

where

$$t_{v,i} = [I_m + R_{\text{PR}}^{-1} H(\sigma_i)]^{-1} R_{\text{PR}}^{-\frac{1}{2}}, \quad (89)$$

$$t_{w,i} = [I_p + R_{\text{PR}}^{-1} H^*(\mu_i)]^{-1} R_{\text{PR}}^{-\frac{1}{2}}. \quad (90)$$

For DD-BR-BT:

$$Q_v^{-1} \approx \text{blkdiag}(2\text{Real}(\sigma_1)[I_m - t_{v,1}^* H^*(\sigma_1) R_p^{-1} H(\sigma_1) t_{v,1}]^{-1}, \dots, \\ 2\text{Real}(\sigma_v)[I_m + t_{v,v}^* H^*(\sigma_v) R_p^{-1} H(\sigma_v) t_{v,v}]^{-1}), \quad (91)$$

$$P_w^{-1} \approx \text{blkdiag}(2\text{Real}(\mu_1)[I_p - t_{w,1}^* H(\mu_1) R_q^{-1} H^*(\mu_1) t_{w,1}]^{-1}, \dots, \\ 2\text{Real}(\mu_w)[I_p - t_{w,w}^* H(\mu_w) R_q^{-1} H^*(\mu_w) t_{w,w}]^{-1}), \quad (92)$$

$$T_v \approx \text{blkdiag}(t_{v,1}, \dots, t_{v,v}), \quad (93)$$

$$T_w \approx \text{blkdiag}(t_{w,1}, \dots, t_{w,w}), \quad (94)$$

where

$$t_{v,i} = [I_m - D^T R_p^{-1} H(\sigma_i)]^{-1} R_b^{\frac{1}{2}}, \quad (95)$$

$$t_{w,i} = [I_p - D R_q^{-1} H^*(\mu_i)]^{-1} R_c^{\frac{1}{2}}. \quad (96)$$

For DD-SW-BT:

$$Q_v^{-1} \approx \text{blkdiag}(2\text{Real}(\sigma_1)I_m, \dots, 2\text{Real}(\sigma_v)I_m), \quad (97)$$

$$P_w^{-1} \approx \text{blkdiag}(2\text{Real}(\mu_1)I_p, \dots, 2\text{Real}(\mu_w)I_p), \quad (98)$$

$$T_w \approx \text{blkdiag}([G(\mu_1)]^{-*}, \dots, [G(\mu_w)]^{-*}). \quad (99)$$

For DD-BST:

$$Q_v^{-1} \approx \text{blkdiag}(2\text{Real}(\sigma_1)I_m, \dots, 2\text{Real}(\sigma_v)I_m), \quad (100)$$

$$P_w^{-1} \approx \text{blkdiag}(2\text{Real}(\mu_1)[I_p - t_{w,1}^* \mathcal{H}(\mu_1) R_X^{-1} \mathcal{H}^*(\mu_1) t_{w,1}]^{-1}, \dots, \\ 2\text{Real}(\mu_w)[I_p - t_{w,w}^* \mathcal{H}(\mu_w) R_X^{-1} \mathcal{H}^*(\mu_w) t_{w,w}]^{-1}), \quad (101)$$

$$T_w \approx \text{blkdiag}(t_{w,1}, \dots, t_{w,w}), \quad (102)$$

where

$$\mathcal{H}(\mu_i) = \begin{cases} \frac{2\text{Real}(\sigma_i)}{\mu_i - \sigma_i} [H(\sigma_i) - H(\mu_i)] H^*(\sigma_i) + H(\mu_i) D^T & \text{if } \sigma_i \neq \mu_i \\ 2\text{Real}(\sigma_i) H'(\sigma_i) H^*(\sigma_i) + H(\mu_i) D^T & \text{if } \sigma_i = \mu_i \end{cases}, \quad (103)$$

$$t_{w,i} = [R_X + \mathcal{H}^*(\mu_i)]^{-1} R_X^{\frac{1}{2}}. \quad (104)$$

Using these formulas, the algorithms proposed in this paper can be efficiently implemented. Even if samples of  $G(s)$  are available along the  $j\omega$ -axis, one can set a near-zero damping value and still use the above formulas and algorithms without significant loss of accuracy.

#### 4. Numerical Results

We present two numerical examples. The first is an illustrative example designed to facilitate convenient verification of the key theoretical results presented in the paper. The second is a modest-order RLC circuit model, which demonstrates the performance of the algorithms in a practical setting. For the state-space matrices of the RLC circuit, refer to [3]. The MATLAB codes for reproducing the results of both examples are provided in the Appendices. Readers only need to run these codes to replicate the results presented in this section.

All necessary accompanying MATLAB functions are also included in the Appendices. All simulations were conducted in MATLAB R2021b on a laptop with a 2 GHz Intel i7 processor and 16 GB of RAM.

#### 4.1. Example 1: Illustrative Example

Consider the following 8<sup>th</sup>-order system with 2 inputs and 2 outputs:

$$\begin{aligned}
 A &= \begin{bmatrix} -1.7126 & 0.8101 & 0.4490 & -0.0665 & -0.7850 & -0.7015 & -0.1898 & 0.5004 \\ 0.8101 & -2.2155 & -0.2692 & 0.3775 & 0.9095 & 0.4206 & 0.4722 & -0.6070 \\ 0.4490 & -0.2692 & -1.2961 & -0.0875 & -0.1553 & 0.4107 & -0.0627 & 0.0416 \\ -0.0665 & 0.3775 & -0.0875 & -0.8279 & -0.1431 & 0.3780 & 0.1840 & 0.1695 \\ -0.7850 & 0.9095 & -0.1553 & -0.1431 & -1.9389 & -0.6784 & -0.6228 & 1.0619 \\ -0.7015 & 0.4206 & 0.4107 & 0.3780 & -0.6784 & -1.6593 & -0.4140 & 0.2694 \\ -0.1898 & 0.4722 & -0.0627 & 0.1840 & -0.6228 & -0.4140 & -1.3181 & 0.5562 \\ 0.5004 & -0.6070 & 0.0416 & 0.1695 & 1.0619 & 0.2694 & 0.5562 & -1.4047 \end{bmatrix}, \\
 B &= \begin{bmatrix} 0.5936 & 0 \\ 0 & 0.4608 \\ -0.3270 & 0 \\ 0.4523 & 0.1748 \\ 0.3379 & -0.1452 \\ 0.2104 & 0 \\ 0.0376 & -0.4913 \\ -0.3827 & 0 \end{bmatrix}, \\
 C &= \begin{bmatrix} -0.2573 & 0.2372 & -0.1253 & 0 & 0 & 0.1977 & -0.1448 & -0.5704 \\ 0 & 0.3321 & -0.1056 & -0.5248 & 0.1269 & -0.4520 & -0.7193 & -0.5483 \end{bmatrix}, \\
 D &= \begin{bmatrix} 0.0708 & 0.0584 \\ 0.0382 & 0.1167 \end{bmatrix}.
 \end{aligned}$$

This model is stable, minimum phase, positive-real, and bounded-real, allowing all the algorithms presented in this paper to be verified. The interpolation points used for the algorithms are:  $(\sigma_1, \sigma_2) = (\mu_1, \mu_2) = (0.5, 0.7)$ .

The step responses of the closed-loop system with 4<sup>th</sup>-order LQG and  $\mathcal{H}_\infty$  controllers—designed using DD-LQG-BT and DD- $\mathcal{H}_\infty$ -BT—are plotted in Figures 1 and 2. The responses match those of the closed-loop system with 8<sup>th</sup>-order intrusively designed LQG and  $\mathcal{H}_\infty$  controllers. By running the MATLAB code in the Appendix A, readers can reproduce the output given in Appendix D, verifying most of the theoretical results in the paper.

#### 4.2. Example 2: RLC Circuit

This model is taken from [3]. The performance of the proposed non-intrusive algorithms is evaluated following the same comparison methodology as in [3]. By running the MATLAB code provided in Appendix B, readers can generate plots demonstrating that the non-intrusive implementations successfully capture all dominant Hankel-like singular values.

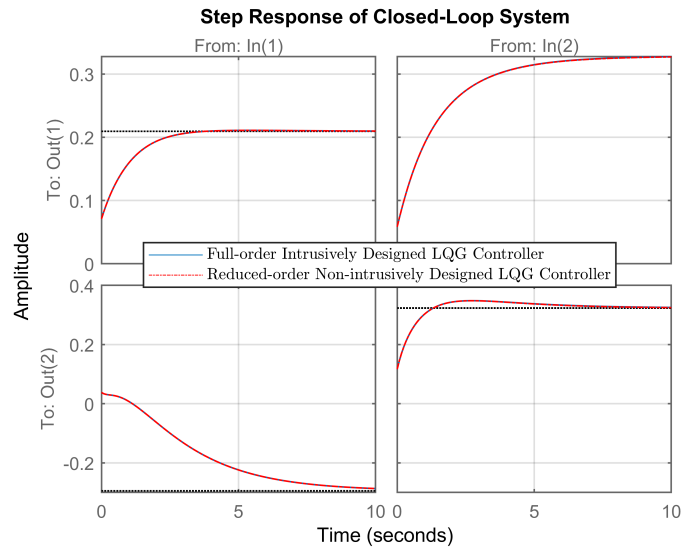


Figure 1: Performance Comparison of the LQG Controller

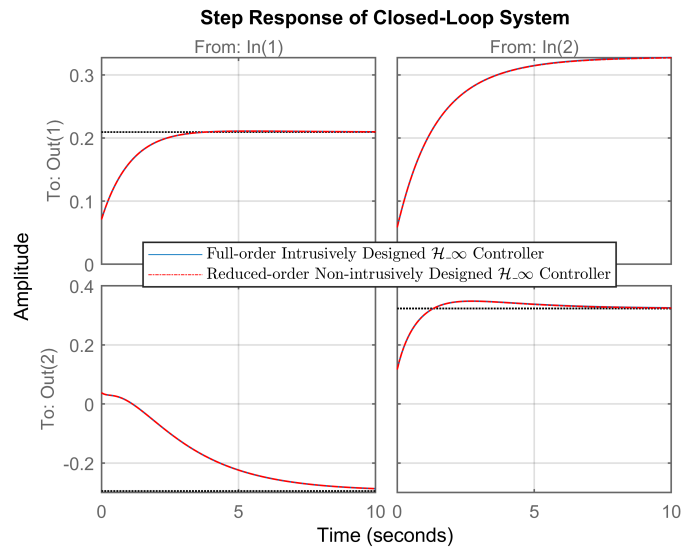


Figure 2: Performance Comparison of the  $\mathcal{H}_\infty$  Controller

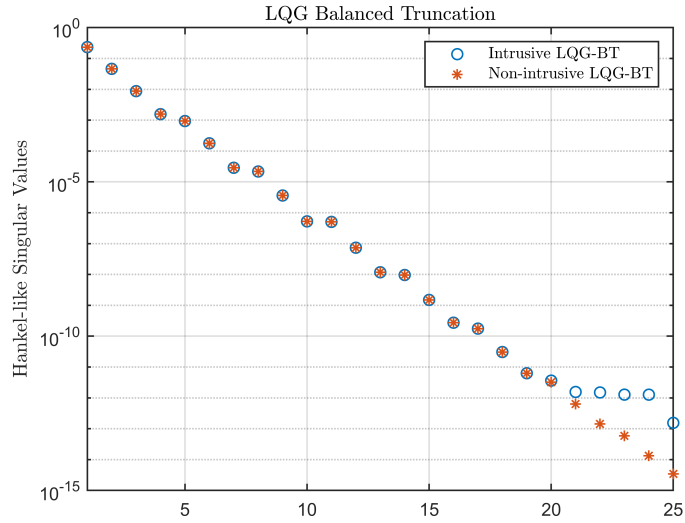


Figure 3: Performance Comparison of LQG-BT

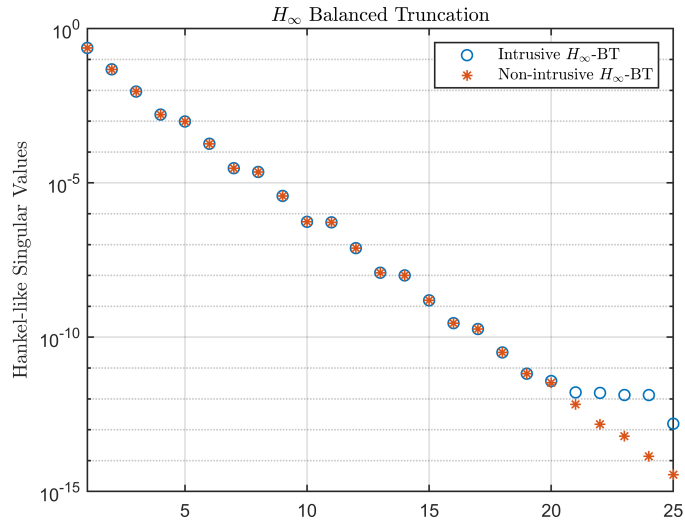


Figure 4: Performance Comparison of  $\mathcal{H}_\infty$ -BT

## 5. Conclusion

This paper presents an interpolation-based implementation of the RADI algorithm for approximating large-scale Riccati equations. Building on this

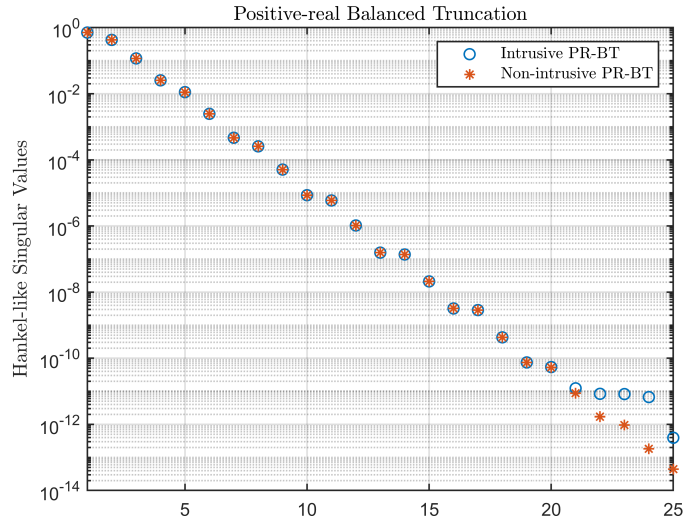


Figure 5: Performance Comparison of PR-BT

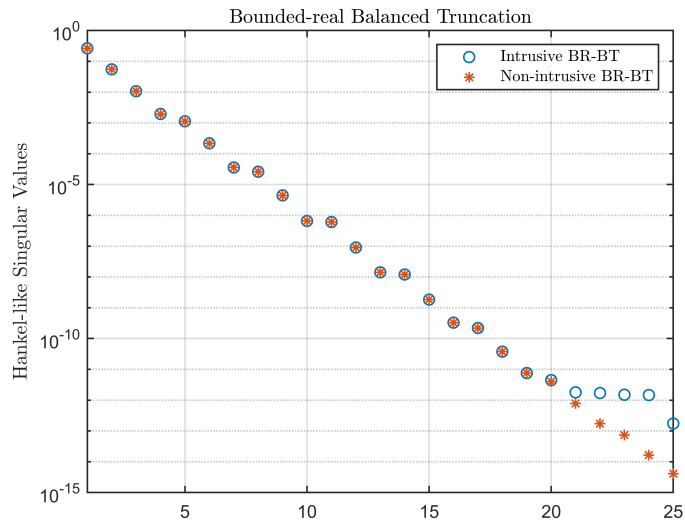


Figure 6: Performance Comparison of BR-BT

foundation, we propose several data-driven interpolation algorithms that preserve critical system properties, including positive-realness, bounded-realness,

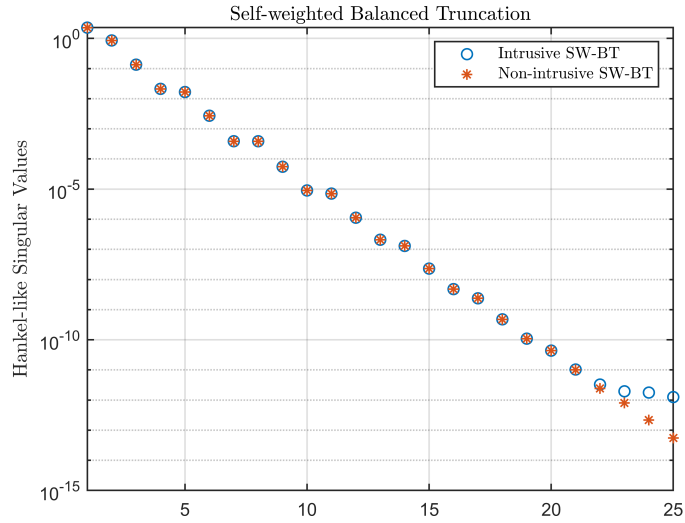


Figure 7: Performance Comparison of SW-BT

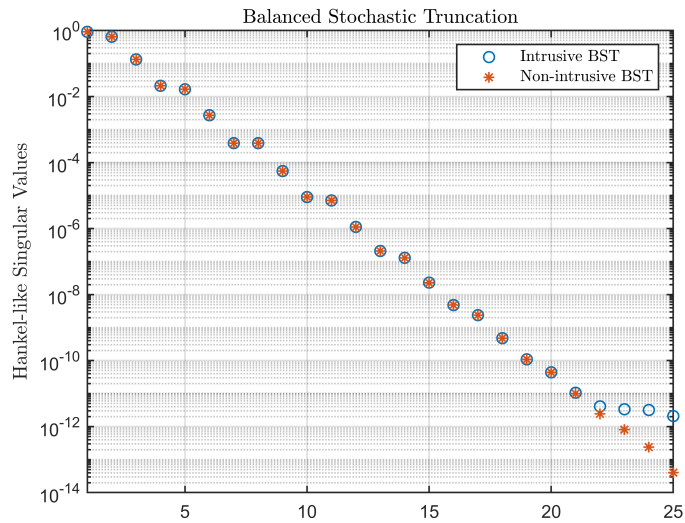


Figure 8: Performance Comparison of BST

and minimum-phase characteristics. Furthermore, we develop data-driven implementations of LQG-BT and  $\mathcal{H}_\infty$ -BT, enabling the design of LQG and  $\mathcal{H}_\infty$

controllers for plants without requiring state-space realizations. We also introduce data-driven versions of PR-BT, BR-BT, SW-BT, and BST algorithms. The paper addresses potential numerical implementation challenges and provides effective solutions. Numerical experiments demonstrate that the proposed algorithms achieve performance comparable to their intrusive counterparts.

### Acknowledgment

We are deeply grateful to Ion Victor Gosea at the Max Planck Institute for Dynamics of Complex Technical Systems in Magdeburg, Germany, for his patient responses to our numerous questions about the Loewner framework and for his valuable feedback. We are also thankful to Prof. Patrick Kürschner at Leipzig University of Applied Sciences for his patient responses to our numerous questions about ADI method.

### Appendix A: MATLAB Codes for Example 1

```
clc
clear
close all

%% Initialization

A =[-1.7126    0.8101    0.4490   -0.0665   -0.7850   -0.7015   -0.1898    0.5004;
     0.8101   -2.2155   -0.2692    0.3775    0.9095    0.4206    0.4722   -0.6070;
     0.4490   -0.2692   -1.2961   -0.0875   -0.1553    0.4107   -0.0627    0.0416;
    -0.0665    0.3775   -0.0875   -0.8279   -0.1431    0.3780    0.1840    0.1695;
    -0.7850    0.9095   -0.1553   -0.1431   -1.9389   -0.6784   -0.6228    1.0619;
    -0.7015    0.4206    0.4107    0.3780   -0.6784   -1.6593   -0.4140    0.2694;
    -0.1898    0.4722   -0.0627    0.1840   -0.6228   -0.4140   -1.3181    0.5562;
     0.5004   -0.6070    0.0416    0.1695    1.0619    0.2694    0.5562   -1.4047];
```

```

B =[0.5936      0;
    0      0.4608;
   -0.3270      0;
    0.4523      0.1748;
    0.3379     -0.1452;
    0.2104      0;
    0.0376     -0.4913;
   -0.3827      0];

C =[-0.2573    0.2372   -0.1253      0      0    0.1977   -0.1448   -0.5704;
    0      0.3321   -0.1056   -0.5248    0.1269   -0.4520   -0.7193   -0.5483];
D =[0.0708    0.0584;
    0.0382    0.1167];

G=ss(A,B,C,D);

[n,m]=size(B); p=size(C,1);
Im=eye(m); Ip=eye(p); I=eye(n);

s=[0.5 0.7]; % Right Interpolation points
u=[0.5 0.7]; % Left Interpolation points
ns=length(s); nu=length(u);

Sv=kron(diag(s),Im); Lv=kron(ones(1,ns),Im);
Sw=kron(diag(u),Ip); Lw=kron(ones(nu,1),Ip);

[Gs,Gu,Gd] = gen_data_trip(I,A,B,C,s,s); % Generates Data
[WTV,WTAV,WTB,CV] = blk_Loewner(Gs,Gu,Gd,s,s); % Constructs Loewner Quadruplet

r=2; % Reduced Order

```

```

%% Non-intrusive Data-driven LQG Controller Design
disp('Now verifying properties of LQG Balanced Truncation...')
disp('Verifying that  $Q_v^{-1}$  and  $\hat{P}_{LQG}$  are the same')
Qv=lyap(-Sv',Lv'*Lv+CV'*CV); Pr=inv(Qv)
care((Sv-Pr*Lv'*Lv)', CV', Pr*Lv'*Lv*Pr)
disp('See! It is identical')
disp('Verifying that  $P_w^{-1}$  and  $\hat{Q}_{LQG}$  are the same')
Pw=lyap(-Sw,Lw*Lw'+WTB*WTB'); Qr=inv(Pw)
care(Sw-Lw*Lw'*Qr, WTB, Qr*Lw*Lw'*Qr)
disp('See! It is identical')
Lp = my_chol(Pr); Lq = my_chol(Qr);
[Ar,Br,Cr] = bsq(WTV,WTAV,WTB,CV,Lp,Lq,r);
[Ac,Bc,Cc,Dc] = design_lqg(A,B,C,D);
lqg_controller=ss(Ac,Bc,Cc,Dc);
closed_loop = feedback(G, lqg_controller);
[Acr,Bcr,Ccr,Dcr] = design_lqg(Ar,Br,Cr,D);
reduced_lqg_controller=ss(Acr,Bcr,Ccr,Dcr);
reduced_closed_loop = feedback(G, reduced_lqg_controller);

figure(1)
step(closed_loop, 10); % Step response
hold on
step(reduced_closed_loop, 10,'r-.'); % Step response
title('Step Response of Closed-Loop System');
grid on;
legend('Full-order Intrusively Designed LQG Controller','Reduced-order Non-intrusively Design')

%% Non-intrusive Data-driven H infinity Controller Design
disp('Now verifying properties of H Infinity Balanced Truncation...')
gm=2; rho=1-gm^-2;
disp('Verifying that  $Q_v^{-1}$  and  $\hat{P}_{H_\infty}$  are the same')

```

```

Qv=lyap(-Sv',Lv'*Lv+rho*CV'*CV); Pr=inv(Qv)
care((Sv-Pr*Lv'*Lv)', sqrt(rho)*CV', Pr*Lv'*Lv*Pr)
disp('See! It is identical')
disp('Verifying that P_w^{-1} and \hat{Q}_H_{\infty} are the same')
Pw=lyap(-Sw,Lw*Lw'+rho*WTB*WTB'); Qr=inv(Pw)
care(Sw-Lw*Lw'*Qr, sqrt(rho)*WTB, Qr*Lw*Lw'*Qr)
disp('See! It is identical')
Lp = my_chol(Pr); Lq = my_chol(Qr);
[Ar,Br,Cr] = bsq(WTV,WTAV,WTB,CV,Lp,Lq,r);
[Ac,Bc,Cc,Dc] = design_h_inf(A,B,C,D,gm);
h_inf_controller=ss(Ac,Bc,Cc,Dc);
closed_loop = feedback(G, h_inf_controller);
[Acr,Bcr,Ccr,Dcr] = design_h_inf(Ar,Br,Cr,D,gm);
reduced_h_inf_controller=ss(Acr,Bcr,Ccr,Dcr);
reduced_closed_loop = feedback(G, reduced_h_inf_controller);

figure(2)
step(closed_loop, 10); % Step response
hold on
step(reduced_closed_loop, 10,'r-.'); % Step response
title('Step Response of Closed-Loop System');
grid on;
legend('Full-order Intrusively Designed  $\mathcal{H}_{\infty}$  Controller','Reduced-order N

%% Positive-realness Preserving Interpolation (V-type)
disp('Now verifying properties of positive-realness preserving interpolation (V-type)...')
R=D+D';
qv=lyap(-Sv',Lv'*Lv); qvi=inv(qv);
Tv=lyap(Sv-qvi*Lv'*Lv-qvi*Lv'*inv(R)*CV,-Sv,qvi*Lv'*(R^-0.5)*Lv);
Qv=lyap(-Sv',Lv'*Lv-Tv'*CV'*inv(R)*CV*Tv);
disp('Verifying that Q_v^{-1} and \hat{P}_{PR} are the same')

```

```

Qvi=inv(Qv)

% Realization No # 1
Ar=Sv-Qvi*Lv'*Lv+Qvi*Lv'*(R^-0.5)*CV*Tv;
Br=Qvi*Lv'*sqrtm(R);
Cr=CV*Tv;
pr_ricc_P(Ar,Br,Cr,D)
disp('See! It is identical')

disp('Now checking if it is passive')
Gr=ss(Ar,Br,Cr,D);
isPassive(Gr)
disp('See! It is passive')

% Realization No # 2
disp('Now let us see if the second realization is passive')
Cr=CV;
Br=Tv*Qvi*Lv'*sqrtm(R);
Ar=Sv-Br*Lv;
Gr1=ss(Ar,Br,Cr,D);
isPassive(Gr1)
disp('See! It is passive')
disp('Now let us see if it satisfies the interpolation conditions')
Ir=eye(size(Ar));
C*inv(s(1)*I-A)*B
Cr*inv(s(1)*Ir-Ar)*Br

C*inv(s(2)*I-A)*B
Cr*inv(s(2)*Ir-Ar)*Br
disp('See! It satisfy interpolation conditions')

```

```

disp('Now see the Hankel singular values of these two realizations to verify these two are identical')
Hankel_singular_values_of_Realization_1=hsvd(Gr)
Hankel_singular_values_of_Realization_2=hsvd(Gr1)
disp('See! These two are identical models')
%% Positive-realness Preserving Interpolation (W-type)
disp('Now verifying properties of positive-realness preserving interpolation (W-type)...')
pw=lyap(-Sw,Lw*Lw'); pwi=inv(pw);
Tw=lyap((Sw-Lw*Lw'*pwi-WTB*inv(R)*Lw'*pwi)',-Sw',pwi*Lw*(R^-0.5)*Lw');
Pw=lyap(-Sw,Lw*Lw'-Tw'*WTB*inv(R)*WTB'*Tw);
disp('Verifying that P_w^{-1} and \hat{Q}_PR are the same')
Pwi=inv(Pw)

% Realization No. 1
Ar=Sw-Lw*Lw'*Pwi+Tw'*WTB*(R^-0.5)*Lw'*Pwi;
Br=Tw'*WTB;
Cr=sqrtm(R)*Lw'*Pwi;
pr_ricc_Q(Ar,Br,Cr,D)
disp('See! It is identical')

disp('Now checking if it is passive')
Gr=ss(Ar,Br,Cr,D);
isPassive(Gr)
disp('See! It is passive')

% Realization No. 2
disp('Now let us see if the second realization is passive')
Br=WTB;
Cr=sqrtm(R)*Lw'*Pwi*Tw';
Ar=Sw-Lw*Cr;

Gr1=ss(Ar,Br,Cr,D);

```

```

isPassive(Gr1)
disp('See! It is passive')
disp('Now let us see if it satisfies the interpolation conditions')
Ir=eye(size(Ar));
C*inv(s(1)*I-A)*B
Cr*inv(s(1)*Ir-Ar)*Br

C*inv(s(2)*I-A)*B
Cr*inv(s(2)*Ir-Ar)*Br
disp('See! It satisfy interpolation conditions')

disp('Now see the Hankel singular values of these two realizations to verify these two are identical')
Hankel_singular_values_of_Realization_1=hsvd(Gr)
Hankel_singular_values_of_Realization_2=hsvd(Gr1)
disp('See! These two are identical models')

%% Positive-real Balanced Truncation
disp('Now verifying properties of Positive-real Balanced Truncation....')
disp('Starting with Intrusive Positive-real Balanced Truncation....')
% Intrusive PRBT
P = pr_ricc_P(A,B,C,D);
Q = pr_ricc_Q(A,B,C,D);
Lp = my_chol(P); Lq= my_chol(Q);
[Ar,Br,Cr] = bsq(I,A,B,C,Lp,Lq,r);
Gr=ss(Ar,Br,Cr,D);
disp('Verifying that Intrusive PRBT produced a passive model')
isPassive(Gr)
disp('It is indeed passive')
Pr = pr_ricc_P(Ar,Br,Cr,D);
Qr = pr_ricc_Q(Ar,Br,Cr,D);
zp = my_chol(Pr); zq = my_chol(Qr);

```

```

disp('Now checking the (HANKEL-LIKE) singular values')
svd(zq'*zp)
disp('Now moving to Non-intrusive Positive-real Balanced Truncation...')
% Non-intrusive PRBT
qv=lyap(-Sv',Lv'*Lv); qvi=inv(qv);
Tv=lyap(Sv-qvi*Lv'*Lv-qvi*Lv'*inv(R)*CV,-Sv,qvi*Lv'*(R^-0.5)*Lv);
Qv=lyap(-Sv',Lv'*Lv-Tv'*CV'*inv(R)*CV*Tv); Qvi=inv(Qv);

pw=lyap(-Sw,Lw*Lw'); pwi=inv(pw);
Tw=lyap((Sw-Lw*Lw'*pwi-WTB*inv(R)*Lw'*pwi)',-Sw',pwi*Lw'*(R^-0.5)*Lw');
Pw=lyap(-Sw,Lw*Lw'-Tw'*WTB*inv(R)*WTB'*Tw); Pwi=inv(Pw);

Lp = my_chol(Qvi); Lq= my_chol(Pwi);
[Ar,Br,Cr] = bsq(WTV,WTAV,WTB,CV,Tv*Lp,Tw*Lq,r);

Pr = pr_ricc_P(Ar,Br,Cr,D);
Qr = pr_ricc_Q(Ar,Br,Cr,D);
disp('Verifying that Non-intrusive PRBT produced a passive model')
Gr1=ss(Ar,Br,Cr,D);
isPassive(Gr1)
disp('It is indeed passive')
zp = my_chol(Pr); zq = my_chol(Qr);
svd(zq'*zp)
disp('Now checking the (HANKEL-LIKE) singular values')
disp('These are close to that of the ROM produced by Intrusive PRBT')

%% Bounded-realness Preserving Interpolation (V-type)
Rp=Ip-D*D'; Rq=Im-D'*D; Rb=Im+D'*inv(Rp)*D; Rc=Ip+D*inv(Rq)*D';
disp('Now verifying properties of bounded-realness preserving interpolation (V-type)...')
qv=lyap(-Sv',Lv'*Lv); qvi=inv(qv);
Tv=lyap(Sv-qvi*Lv'*Lv+qvi*Lv'*D'*inv(Rp)*CV,-Sv,qvi*Lv'*sqrtm(Rb)*Lv);

```

```

disp('Verifying that  $Q_v^{-1}$  and  $\hat{P}_{BR}$  are the same')
Qv=lyap(-Sv',Lv'*Lv-Tv'*CV'*inv(Rp)*CV*Tv); Qvi=inv(Qv)

% Realization No. 1
Br=Qvi*Lv'*(Rb^-0.5); Cr=CV*Tv;
Ar=Sv-Qvi*Lv'*Lv-Br*D'*inv(Rp)*Cr;
br_ricc_P(Ar,Br,Cr,D)
disp('See! It is identical')

disp('Now checking if it is passive')
Gr=ss(Ar,Br,Cr,D);
isPassive(Gr)
disp('See! It is passive')

% Realization No. 2
disp('Now let us see if the second realization is passive')
Br=Tv*Qvi*Lv'*(Rb^-0.5); Cr=CV;
Ar=Sv-Br*Lv;
disp('Now checking if it is passive')
Gr1=ss(Ar,Br,Cr,D);
isPassive(Gr1)
disp('See! It is passive')
disp('Now let us see if it satisfies the interpolation conditions')
Ir=eye(size(Ar));
C*inv(s(1)*I-A)*B
Cr*inv(s(1)*Ir-Ar)*Br

C*inv(s(2)*I-A)*B
Cr*inv(s(2)*Ir-Ar)*Br
disp('See! It satisfy interpolation conditions')

```

```

disp('Now see the Hankel singular values of these two realizations to verify these two are identical')
Hankel_singular_values_of_Realization_1=hsvd(Gr)
Hankel_singular_values_of_Realization_2=hsvd(Gr1)
disp('See! These two are identical models')
%% Bounded-realness Preserving Interpolation (W-type)
disp('Now verifying properties of bounded-realness preserving interpolation (W-type)...')
pw=lyap(-Sw,Lw*Lw'); pwi=inv(pw);
Tw=lyap((Sw-Lw*Lw'*pwi+WTB*inv(Rq)*D'*Lw'*pwi)',-Sw',pwi*Lw*sqrtm(Rc)*Lw');
disp('Verifying that P_w^{-1} and \hat{Q}_BR are the same')
Pw=lyap(-Sw,Lw*Lw'-Tw'*WTB*inv(Rq)*WTB'*Tw); Pwi=inv(Pw)
% Realization No. 1
Br=Tw'*WTB;
Cr=(Rc^-0.5)*Lw'*Pwi;
Ar=Sw-Lw*Lw'*Pwi-Br*inv(Rq)*D'*Cr;
br_ricc_Q(Ar,Br,Cr,D)
disp('See! It is identical')
disp('Now checking if it is passive')
Gr=ss(Ar,Br,Cr,D);
isPassive(Gr)
disp('See! It is passive')

% Realization No. 2
Br=WTB;
Cr=(Rc^-0.5)*Lw'*Pwi*Tw';
Ar=Sw-Lw*Cr;
disp('Now let us see if the second realization is passive')
Gr1=ss(Ar,Br,Cr,D);
isPassive(Gr1)
disp('See! It is passive')
disp('Now let us see if it satisfies the interpolation conditions')

```

```

Ir=eye(size(Ar));
C*inv(s(1)*I-A)*B
Cr*inv(s(1)*Ir-Ar)*Br

C*inv(s(2)*I-A)*B
Cr*inv(s(2)*Ir-Ar)*Br
disp('See! It satisfy interpolation conditions')
disp('Now see the Hankel singular values of these two realizations to verify these two are identical models')
Hankel_singular_values_of_Realization_1=hsvd(Gr)
Hankel_singular_values_of_Realization_2=hsvd(Gr1)
disp('See! These two are identical models')

%% Bounded-real Balanced Truncation
disp('Now verifying properties of Bounded-real Balanced Truncation....')
disp('Starting with Intrusive Bounded-real Balanced Truncation....')
% Intrusive BRBT
P = br_ricc_P(A,B,C,D);
Q = br_ricc_Q(A,B,C,D);
Lp = my_chol(P); Lq= my_chol(Q);
[Ar,Br,Cr] = bsq(I,A,B,C,Lp,Lq,r);
Gr=ss(Ar,Br,Cr,D);
disp('Verifying that Intrusive BRBT produced a passive model')
isPassive(Gr)
disp('It is indeed passive')
Pr = br_ricc_P(Ar,Br,Cr,D);
Qr = br_ricc_Q(Ar,Br,Cr,D);
zp = my_chol(Pr); zq = my_chol(Qr);
disp('Now checking the (HANKEL-LIKE) singular values')
svd(zq'*zp)
disp('Now moving to Non-intrusive Bounded-real Balanced Truncation....')

```

```

% Non-intrusive Bounded-real Balanced Truncation
qv=lyap(-Sv',Lv'*Lv); qvi=inv(qv);
Tv=lyap(Sv-qvi*Lv'*Lv+qvi*Lv'*D'*inv(Rp)*CV,-Sv,qvi*Lv'*sqrtm(Rb)*Lv);
Qv=lyap(-Sv',Lv'*Lv-Tv'*CV'*inv(Rp)*CV*Tv); Qvi=inv(Qv);
pw=lyap(-Sw,Lw*Lw'); pwi=inv(pw);
Tw=lyap((Sw-Lw*Lw'*pwi+WTB*inv(Rq)*D'*Lw'*pwi)',-Sw',pwi*Lw*sqrtm(Rc)*Lw');
Pw=lyap(-Sw,Lw*Lw'-Tw'*WTB*inv(Rq)*WTB'*Tw); Pwi=inv(Pw);

Lp = my_chol(Qvi); Lq= my_chol(Pwi);
[Ar,Br,Cr] = bsq(WTV,WTAV,WTB,CV,Tv*Lp,Tw*Lq,r);

Pr = br_ricc_P(Ar,Br,Cr,D);
Qr = br_ricc_Q(Ar,Br,Cr,D);
disp('Verifying that Non-intrusive BRBT produced a passive model')
Gr1=ss(Ar,Br,Cr,D);
isPassive(Gr1)
disp('It is indeed passive')
zp = my_chol(Pr); zq = my_chol(Qr);
svd(zq'*zp)
disp('Now checking the (HANKEL-LIKE) singular values')
disp('These are close to that of the ROM produced by Intrusive BRBT')

%% Interpolation with Preservation of Minimum Phase Property (Zero Placement)
disp('Now verifying properties of minimum phase preserving interpolation (Zero Placement)...')
Pw=lyap(-Sw,Lw*Lw'); Pwi=inv(Pw);
Tw=lyap((Sw-Lw*Lw'*Pwi-WTB*inv(D)*Lw'*Pwi)',-Sw',Pwi*Lw*inv(D)*Lw');

Cr=D*Lw'*Pwi*Tw';
Br=WTB;
Ar=Sw-Lw*Cr;
disp('Verifying if the zeros are at the mirror images of the interpolation points')

```

```

eig(Ar-Br*inv(D)*Cr)
disp('See! It is minimum phase with zeros at the mirror images of the interpolation points')
disp('Now let us see if it satisfies the interpolation conditions')

Ir=eye(size(Ar));
C*inv(s(1)*I-A)*B
Cr*inv(s(1)*Ir-Ar)*Br

C*inv(s(2)*I-A)*B
Cr*inv(s(2)*Ir-Ar)*Br
disp('See! It satisfy interpolation conditions')

%% Self-weighted Balanced Truncation
disp('Now verifying properties of Self-weighted Balanced Truncation...')
disp('Starting with Intrusive Self-weighted Balanced Truncation...')
% Intrusive SWBT
P=lyap(A,B*B');
Q=lyap((A-B*inv(D)*C)',C'*inv(D*D')*C);
Zp = my_chol(P); Zq = my_chol(Q);
[Ar,Br,Cr] = bsq(I,A,B,C,Zp,Zq,r);
disp('Verifying that SWBT produced a minimum phase model')
eig(Ar-Br*inv(D)*Cr)
disp('It is indeed minimum phase')
Pr=lyap(Ar,Br*Br');
Qr=lyap((Ar-Br*inv(D)*Cr)',Cr'*inv(D*D')*Cr);
zp = my_chol(Pr); zq = my_chol(Qr);
disp('Now checking the (HANKEL-LIKE) singular values')
svd(zq'*zp)

```

```

disp('Now moving to Non-intrusive SWBT....')
% Non-intrusive SWBT
Qv=lyap(-Sv,Lv'*Lv); Qvi=inv(Qv);
Pw=lyap(-Sw,Lw'*Lw'); Pwi=inv(Pw);
Tw=lyap((Sw-Lw*Lw'*Pwi-WTB*inv(D)*Lw'*Pwi)',-Sw',Pwi*Lw*inv(D')*Lw');
Lp = my_chol(Qvi); Lq = my_chol(Pwi);
[Ar,Br,Cr] = bsq(WTV,WTAV,WTB,CV,Lp,Tw*Lq,r);
disp('Verifying that Non-intrusive SWBT produced a minimum phase model')
eig(Ar-Br*inv(D)*Cr)
disp('It is indeed minimum phase')
Pr=lyap(Ar,Br*Br');
Qr=lyap((Ar-Br*inv(D)*Cr)',Cr'*inv(D*D')*Cr);
zp = my_chol(Pr); zq = my_chol(Qr);
disp('Now checking the (HANKEL-LIKE) singular values')
svd(zq'*zp)
disp('These are close to that of the ROM produced by Intrusive SWBT')

%% Balanced Stochastic Truncation
disp('Now verifying properties of Balanced Stochastic Truncation....')
disp('Starting with Intrusive Balanced Stochastic Truncation....')
% Intrusive BST
P=lyap(A,B*B');
Q = bst_ricc_Q(A,B,C,D);
Zp = my_chol(P); Zq = my_chol(Q);
[Ar,Br,Cr] = bsq(I,A,B,C,Zp,Zq,r);
disp('Verifying that BST produced a minimum phase model')
eig(Ar-Br*inv(D)*Cr)
disp('It is indeed minimum phase')
Pr=lyap(Ar,Br*Br');
Qr=bst_ricc_Q(Ar,Br,Cr,D);
zp = my_chol(Pr); zq = my_chol(Qr);

```

```

disp('Now checking the (HANKEL-LIKE) singular values')
svd(zq'*zp)

% Non-intrusive BST
Rx=D*D';
Qv=lyap(-Sv',Lv'*Lv); Qvi=inv(Qv);
pw=lyap(-Sw,Lw*Lw'); pwi=inv(pw);
Tw=lyap((Sw-Lw*Lw'*pwi-((WTV)*Qvi*(CV)'+WTB*D')*inv(Rx)*Lw'*pwi)',-Sw',pwi*Lw*(Rx^-0.5)*Lw');
Bxr=(Tw'*WTV*Qvi*CV'+Tw'*WTB*D')*(Rx^-0.5);
Pw=lyap(-Sw,Lw*Lw'-Bxr*Bxr'); Pwi=inv(Pw);
Lp = my_chol(Qvi); Lq = my_chol(Pwi);

[Ar,Br,Cr] = bsq(WTV,WTAV,WTB,CV,Lp,Tw*Lq,r);
disp('Verifying that Non-intrusive BST produced a minimum phase model')
eig(Ar-Br*inv(D)*Cr)
disp('It is indeed minimum phase')
Pr=lyap(Ar,Br*Br');
Qr=bst_ricc_Q(Ar,Br,Cr,D);
zp = my_chol(Pr); zq = my_chol(Qr);
disp('Now checking the (HANKEL-LIKE) singular values')
svd(zq'*zp)
disp('These are close to that of the ROM produced by Intrusive BST')

```

## Appendix B: MATLAB Codes for Example 2

```

clc
clear
close all

%% Initialization

```

```

load circuit400.mat

G = ss(A, B, C, D);
gamma = norm(G, 'inf'); gamma = 2*gamma;
D = D / gamma; C = C / sqrt(gamma); B = B / sqrt(gamma);
G = ss(A, B, C, D);
A=sparse(A); B=sparse(B); C=sparse(C);
[n,m]=size(B); Im=eye(m); p=size(C,1); Ip=eye(p); I=speye(n);

N=150; k1=-1; k2=4; k=k1:(k2-k1)/(N-1):k2; w=10.^k; jw=1i*w;
jw=[jw conj(jw)]; jw=cplxpair(jw); w=imag(jw);
z=1e-5; % Damping of Interpolation points
s = s_zw(z,w,1); % Sampling points (interpolation points)
u=s;
ns=length(s); nu=length(u);

Sv=kron(diag(s),Im); Lv=kron(ones(1,ns),Im);
Sw=kron(diag(u),Ip); Lw=kron(ones(nu,1),Ip);

[Gs,Gu,Gd] = gen_data_trip(I,A,B,C,s,s); % Generates Data
[WTV,WTAV,WTB,CV] = blk_Loewner(Gs,Gu,Gd,s,s); % Constructs Loewner Quadruplet

r=25; % Reduced Order
A=full(A); B=full(B); C=full(C);

%% LQG-BT

% Intrusive
P = care(A', C', B*B');
Q = care(A, B, C'*C);
Zp = my_chol(P); Zq = my_chol(Q);

```

```

[Ar,Br,Cr] = bsq(I,A,B,C,Zp,Zq,r);
Pr = care(Ar', Cr', Br*Br');
Qr = care(Ar, Br, Cr'*Cr);
zp = my_chol(Pr); zq = my_chol(Qr);
h=svd(zq'*zp);

% Non-intrusive
[Lp,Lq] = lqgbt_chol_fact(A,B,C,s,s);
[Ar,Br,Cr] = bsq(WTV,WTAV,WTB,CV,Lp,Lq,r);
Pr = care(Ar', Cr', Br*Br');
Qr = care(Ar, Br, Cr'*Cr);
zp = my_chol(Pr); zq = my_chol(Qr);
hr=svd(zq'*zp);

figure(1)
semilogy(h,'o')
hold on
semilogy(hr,'*')
xlim([1 r])
ylabel('Hankel-like Singular Values','Interpreter','latex')
title('LQG Balanced Truncation','Interpreter','latex')
legend('Intrusive LQG-BT','Non-intrusive LQG-BT','Interpreter','latex')
box on
grid on

%% H Infinity Balanced Truncation

% Intrusive H_infinity BT

gm=2; rho=1-gm^-2;

```

```

P = care(A', sqrt(rho)*C', B*B');
Q = care(A, sqrt(rho)*B, C'*C);
Zp = my_chol(P); Zq = my_chol(Q);
[Ar,Br,Cr] = bsq(I,A,B,C,Zp,Zq,r);
Pr = care(Ar', sqrt(rho)*Cr', Br*Br');
Qr = care(Ar, sqrt(rho)*Br, Cr'*Cr);
zp = my_chol(Pr); zq = my_chol(Qr);
h=svd(zq'*zp);

% Non-intrusive Hinf-BT

[Lp,Lq] = hinfbt_chol_fact(A,B,C,s,s);
[Ar,Br,Cr] = bsq(WTV,WTAV,WTB,CV,Lp,Lq,r);
Pr = care(Ar', sqrt(rho)*Cr', Br*Br');
Qr = care(Ar, sqrt(rho)*Br, Cr'*Cr);
zp = my_chol(Pr); zq = my_chol(Qr);
hr=svd(zq'*zp);

figure(2)
semilogy(h,'o')
hold on
semilogy(hr,'*')
xlim([1 r])
ylabel('Hankel-like Singular Values','Interpreter','latex')
title('$H_{\infty}$ Balanced Truncation','Interpreter','latex')
legend('Intrusive $H_{\infty}$-BT','Non-intrusive $H_{\infty}$-BT','Interpreter','latex')
box on
grid on

%% Positive-real Balanced Truncation

```

```

% Intrusive PRBT

P = pr_ricc_P(A,B,C,D);
Q = pr_ricc_Q(A,B,C,D);
Zp = my_chol(P); Zq = my_chol(Q);
[Ar,Br,Cr] = bsq(I,A,B,C,Zp,Zq,r);
Pr = pr_ricc_P(Ar,Br,Cr,D);
Qr = pr_ricc_Q(Ar,Br,Cr,D);
zp = my_chol(Pr); zq = my_chol(Qr);
h=svd(zq'*zp);

% Non-intrusive PRBT

[Lp,Tv,Lq,Tw] = prbt_chol_fact(A,B,C,D,s,s);
[Ar,Br,Cr] = bsq(WTV,WTAV,WTB,CV,Tv*Lp,Tw*Lq,r);
Pr = pr_ricc_P(Ar,Br,Cr,D);
Qr = pr_ricc_Q(Ar,Br,Cr,D);
zp = my_chol(Pr); zq = my_chol(Qr);
hr=svd(zq'*zp);

figure(3)
semilogy(h,'o')
hold on
semilogy(hr,'*')
xlim([1 r])
ylabel('Hankel-like Singular Values','Interpreter','latex')
title('Positive-real Balanced Truncation','Interpreter','latex')
legend('Intrusive PR-BT','Non-intrusive PR-BT','Interpreter','latex')
box on

```

```

grid on

%% Bounded-real Balanced Truncation

% Intrusive BR-BT
P = br_ricc_P(A,B,C,D);
Q = br_ricc_Q(A,B,C,D);
Zp = my_chol(P); Zq = my_chol(Q);
[Ar,Br,Cr] = bsq(I,A,B,C,Zp,Zq,r);
Pr = br_ricc_P(Ar,Br,Cr,D);
Qr = br_ricc_Q(Ar,Br,Cr,D);
zp = my_chol(Pr); zq = my_chol(Qr);
h=svd(zq'*zp);

% Non-intrusive BR-BT
[Lp,Tv,Lq,Tw] = brbt_chol_fact(A,B,C,D,s,s);
[Ar,Br,Cr] = bsq(WTV,WTAV,WTB,CV,Tv*Lp,Tw*Lq,r);
Pr = br_ricc_P(Ar,Br,Cr,D);
Qr = br_ricc_Q(Ar,Br,Cr,D);
zp = my_chol(Pr); zq = my_chol(Qr);
hr=svd(zq'*zp);

figure(4)
semilogy(h,'o')
hold on
semilogy(hr,'*')
xlim([1 r])
ylabel('Hankel-like Singular Values','Interpreter','latex')
title('Bounded-real Balanced Truncation','Interpreter','latex')
legend('Intrusive BR-BT','Non-intrusive BR-BT','Interpreter','latex')

```

```

box on
grid on

%% Self-weighted Balanced Truncation

% Intrusive SWBT

P=lyap(A,B*B');
Q=lyap((A-B*inv(D)*C)',C'*inv(D*D')*C);
Zp = my_chol(P); Zq = my_chol(Q);
[Ar,Br,Cr] = bsq(I,A,B,C,Zp,Zq,r);
Pr=lyap(Ar,Br*Br');
Qr=lyap((Ar-Br*inv(D)*Cr)',Cr'*inv(D*D')*Cr);
zp = my_chol(Pr); zq = my_chol(Qr);
h=svd(zq'*zp);

% Non-intrusive SWBT
[Lp,Lq,Tw] = swbt_chol_fact(A,B,C,D,s,s);
[Ar,Br,Cr] = bsq(WTV,WTAV,WTB,CV,Lp,Tw*Lq,r);
Pr=lyap(Ar,Br*Br');
Qr=lyap((Ar-Br*inv(D)*Cr)',Cr'*inv(D*D')*Cr);
zp = my_chol(Pr); zq = my_chol(Qr);
hr=svd(zq'*zp);

figure(5)
semilogy(h,'o')
hold on
semilogy(hr,'*')
xlim([1 r])
ylabel('Hankel-like Singular Values','Interpreter','latex')

```

```

title('Self-weighted Balanced Truncation','Interpreter','latex')
legend('Intrusive SW-BT','Non-intrusive SW-BT','Interpreter','latex')
box on
grid on

%% Balanced Stochastic Truncation

% Intrusive

P=lyap(A,B*B');
Q = bst_ricc_Q(A,B,C,D);
Zp = my_chol(P); Zq = my_chol(Q);
[Ar,Br,Cr] = bsq(I,A,B,C,Zp,Zq,r);
Pr=lyap(Ar,Br*Br');
Qr = bst_ricc_Q(Ar,Br,Cr,D);
zp = my_chol(Pr); zq = my_chol(Qr);
h=svd(zq'*zp);

% Non-intrusive

[Lp,Lq,Tw] = bst_chol_fact(A,B,C,D,s,s);
[Ar,Br,Cr] = bsq(WTV,WTAV,WTB,CV,Lp,Tw*Lq,r);
Pr=lyap(Ar,Br*Br');
Qr = bst_ricc_Q(Ar,Br,Cr,D);
zp = my_chol(Pr); zq = my_chol(Qr);
hr=svd(zq'*zp);

figure(6)

```

```

semilogy(h,'o')
hold on
semilogy(hr,'*')
xlim([1 r])
ylabel('Hankel-like Singular Values','Interpreter','latex')
title('Balanced Stochastic Truncation','Interpreter','latex')
legend('Intrusive BST','Non-intrusive BST','Interpreter','latex')
box on
grid on

```

### Appendix C: Functions Required to Run the Codes (In Alphabetical Order)

```

function [Er,Ar,Br,Cr] = blk_Loewner(Gs,Gu,Gd,s,u)

p=size(Gs,1); nu=length(u); ns=length(s);
nsm=size(Gs,2); m=nsm/ns;
Er=zeros(nu,ns); Ar=zeros(nu,ns);
Br=zeros(nu,m); Cr=zeros(p,ns);

for i=1:length(u)

    ki=(i-1)*m+1; li=i*m;
    Ki=(i-1)*p+1; Li=i*p;
    Br(Ki:Li,:)=Gu(:,ki:li);

    for j=1:length(s)

        kj=(j-1)*m+1; lj=j*m;

```

```

if u(i)==s(j)

    Er(Ki:Li,kj:lj)=-Gd(:,kj:lj);
    Ar(Ki:Li,kj:lj)=-Gs(:,kj:lj)+s(j)*Gd(:,kj:lj));

else

    Er(Ki:Li,kj:lj)=(Gs(:,kj:lj)-Gu(:,ki:li))/(u(i)-s(j));

    Ar(Ki:Li,kj:lj)=(s(j)*Gs(:,kj:lj)-u(i)*Gu(:,ki:li))/(u(i)-s(j));

end

Cr(:,kj:lj)=Gs(:,kj:lj);

end

end

end

function [P] = br_ricc_P(A,B,C,D)

```

```

[p,n]=size(C); I=eye(n); Ip=eye(p);
Rp=-(Ip-D*D');
P = icare(A',C',B*B',Rp,B*D',I,0);

end

function [Q] = br_ricc_Q(A,B,C,D)

[n,m]=size(B); I=eye(n); Im=eye(m);
Rq=-(Im-D'*D);
Q = icare(A,B,C'*C,Rq,C'*D,I,0);

end

function [Lp,Tv,Lq,Tw] = brbt_chol_fact(A,B,C,D,s,u)

ns=length(s); nu=length(u);
[n,m]=size(B); p=size(C,1); Im=eye(m); Ip=eye(p); I=speye(n);
Lp=[]; Lq=[];
Rp=Ip-D*D'; Rq=Im-D'*D; Rb=Im+D'*inv(Rp)*D; Rc=Ip+D*inv(Rq)*D';
Tv=[]; Tw=[];

for i=1:ns

    hsi=C*((s(i)*I-A)\B);
    tvi=inv(Im-D'*inv(Rp)*hsi)*(Rb^0.5);
    qvi=2*real(s(i))*inv(Im-tvi'*hsi'*inv(Rp)*hsi*tvi);
    lp = my_chol(qvi);
    Lp=blkdiag(Lp,lp);
    Tv=blkdiag(Tv,tvi);

end

```

```

for i=1:nu

    hui=C*((u(i)*I-A)\B);
    twi=inv(Ip-D'*inv(Rq)*hui')*(Rc^0.5);
    pwi=2*real(u(i))*inv(Ip-twi'*hui*inv(Rq)*hui'*twi);
    lq = my_chol(pwi);
    Lq=blkdiag(Lq,lq);
    Tw=blkdiag(Tw,twi);

end

end

function [Ar,Br,Cr] = bsq(E,A,B,C,Lp,Lq,r)

[Z,S,Y]=svd(Lq'*E*Lp);

S1=S(1:r,1:r); Z1=Z(:,1:r); Y1=Y(:,1:r);

W=(Lq*Z1)/(sqrtm(S1)); V=(Lp*Y1)/(sqrtm(S1));
Ar=W'*A*V; Br=W'*B; Cr=C*V;

end

function [Lp,Lq,Tw] = bst_chol_fact(A,B,C,D,s,u)

ns=length(s); nu=length(u);
[n,m]=size(B); p=size(C,1); Im=eye(m); Ip=eye(p); Ispeye(n);
Lp=[]; Lq=[]; Rx=D*D'; Tw=[];

```

```

for i=1:ns

    lp = sqrt(2*real(s(i)))*Im;
    Lp=blkdiag(Lp,lp);

end

for i=1:nu

    hui=C*((u(i)*I-A)\B);
    hsi=C*((s(i)*I-A)\B);

    if u(i)==s(i)

        ei=(C/(u(i)*I-A))*((u(i)*I-A)\B);

    else

        ei=(hsi-hui)/(u(i)-s(i));

    end

    gui=2*real(s(i))*ei*hsi'+hui*D';
    twi=inv(Rx+gui')*(Rx^0.5);

    pwi=2*real(u(i))*inv(Ip-twi'*gui*inv(Rx)*gui'*twi);
    lq = my_chol(pwi);
    Lq=blkdiag(Lq,lq);
    Tw=blkdiag(Tw,twi);

end

```

```

end

function [Q] = bst_ricc_Q(A,B,C,D)

P=lyap(A,B*B');
Bw=P*C'+B*D';
Ax=A-Bw*inv(D*D')*C;
Q=care(Ax,Bw,C'*inv(D*D')*C,-D*D');

end

function [Ac,Bc,Cc,Dc] = design_h_inf(A,B,C,D,gm)

rho=1-gm^-2;
Q = care(A, sqrt(rho)*B, C'*C);
K=B'*Q;

P = care(A', sqrt(rho)*C', B*B');
L = P * C';

Ac = A - B*K - L*C + L*D*K;
Bc = L;
Cc = -K;
Dc = zeros(size(B,2), size(C,1));

end

function [Ac,Bc,Cc,Dc] = design_lqg(A,B,C,D)

```

```

Q = care(A, B, C'*C);
K=B'*Q;

P = care(A', C', B*B');
L = P * C';

Ac = A - B*K - L*C + L*D*K;
Bc = L;
Cc = -K;
Dc = zeros(size(B,2), size(C,1));

end

function [Gs,Gu,Gd] = gen_data_trip(E,A,B,C,s,u)

ns=length(s); nu=length(u);
m=size(B,2); p=size(C,1);
Gs=zeros(p,m*ns); Gd=Gs;
Gu=zeros(p,m*nu);

for i=1:nu

    ui=u(i); ki=(i-1)*m+1; li=i*m;

    Gu(:,ki:li)=C*((ui*E-A)\B);

    for j=1:ns

        sj=s(j); kj=(j-1)*m+1; lj=j*m;

```

```

Gs(:,kj:lj)=C*((sj*E-A)\B);

if sj==ui

    Gd(:,kj:lj)=-(C/(sj*E-A))*E*((sj*E-A)\B);
end

end

end

end

function [Lp,Lq] = hinfbt_chol_fact(A,B,C,s,u,gm)

ns=length(s); nu=length(u);
[n,m]=size(B); p=size(C,1); Im=eye(m); Ip=eye(p); I=speye(n);
Lp=[]; Lq=[];
gm=2; rho=1-gm^-2;

for i=1:ns

    hsi=C*((s(i)*I-A)\B);
    qvi=2*real(s(i))*inv(Im+rho*hsi'*hsi);
    lp = my_chol(qvi);
    Lp=blkdiag(Lp,lp);

```

```

end

for i=1:nu

    hui=C*((u(i)*I-A)\B);
    pwi=2*real(u(i))*inv(Ip+rho*hui*hui');
    lq = my_chol(pwi);
    Lq=blkdiag(Lq,lq);

end

end

function [Lp,Lq] = lqgbt_chol_fact(A,B,C,s,u)

ns=length(s); nu=length(u);
[n,m]=size(B); p=size(C,1); Im=eye(m); Ip=eye(p); I=speye(n);
Lp=[]; Lq=[];

for i=1:ns

    hsi=C*((s(i)*I-A)\B);
    qvi=2*real(s(i))*inv(Im+hsi'*hsi);
    lp = my_chol(qvi);
    Lp=blkdiag(Lp,lp);

end

for i=1:nu

```

```

    hui=C*((u(i)*I-A)\B);
    pwi=2*real(u(i))*inv(Ip+hui*hui');
    lq = my_chol(pwi);
    Lq=blkdiag(Lq,lq);

end

end

function [Zp] = my_chol(P)

[up,sp,~]=svd(P);
Zp=up*sqrtm(sp);

end

function [P] = pr_ricc_P(A,B,C,D)

R=-(D+D');
P = icare(A',-C',0,R,B,eye(size(A)),0);
Rp=D+D';

end

function [Q] = pr_ricc_Q(A,B,C,D)

R=-(D+D');
Q = icare(A,-B,0,R,C',eye(size(A)),0);
Rp=(D+D');

```

```

end

function [Lp,Tv,Lq,Tw] = prbt_chol_fact(A,B,C,D,s,u)

ns=length(s); nu=length(u);
[n,m]=size(B); p=size(C,1); Im=eye(m); Ip=eye(p); I=speye(n);
Lp=[]; Lq=[]; Rpr=D+D'; Tv=[]; Tw=[];

for i=1:ns

    hsi=C*((s(i)*I-A)\B);
    tvi=inv(Im+inv(Rpr)*hsi)*(Rpr^-0.5);
    qvi=2*real(s(i))*inv(Im-tvi'*hsi'*inv(Rpr)*hsi*tvi);
    lp = my_chol(qvi);
    Lp=blkdiag(Lp,lp);
    Tv=blkdiag(Tv,tvi);

end

for i=1:nu

    hui=C*((u(i)*I-A)\B);
    twi=inv(Im+inv(Rpr)*hui')*(Rpr^-0.5);
    pwi=2*real(u(i))*inv(Ip-twi'*hui*inv(Rpr)*hui'*twi);
    lq = my_chol(pwi);
    Lq=blkdiag(Lq,lq);
    Tw=blkdiag(Tw,twi);

end

```

```

end

function [s,Lp,S,L,Qsi] = s_zw(z,w,m)

s=[]; Lp=[]; Im=eye(m); Qsi=[]; S=[]; L=[]; weights=[];

for k=1:length(w)

s1=((z*abs(w(k)))/sqrt(1-z^2))+j*w(k);
s=[s s1];

end

for k=1:length(s)

S=blkdiag(S,s(k)*Im);
L=[L Im];

qsi=2*real(s(k))*Im;
Qsi=blkdiag(Qsi,qsi);

lp=sqrt(2*real(s(k)))*Im;
Lp=blkdiag(Lp,lp);

end

end

```

```

function [Lp,Lq,Tw] = swbt_chol_fact(A,B,C,D,s,u)

ns=length(s); nu=length(u);
[n,m]=size(B); p=size(C,1); Im=eye(m); Ip=eye(p); I=speye(n);
Lp=[]; Lq=[]; Tw=[];

for i=1:ns

    lp=sqrt(2*real(s(i)));
    Lp=blkdiag(Lp,lp*Im);

end

for i=1:nu

    hui=C*((u(i)*I-A)\B)+D;

    lq = sqrt(2*real(u(i)))*Ip;
    Lq=blkdiag(Lq,lq);
    twi=inv(hui');
    Tw=blkdiag(Tw,twi);

end

end

```

## Appendix D

Now verifying properties of LQG Balanced Truncation....

Verifying that  $Q_v^{-1}$  and  $\hat{P}_{LQG}$  are the same

Pr =

34.3622	0.2108	-40.1977	-0.1323
0.2108	33.4328	-0.2810	-39.1959
-40.1977	-0.2810	48.4087	0.1949
-0.1323	-39.1959	0.1949	47.2950

ans =

34.3622	0.2108	-40.1977	-0.1323
0.2108	33.4328	-0.2810	-39.1959
-40.1977	-0.2810	48.4087	0.1949
-0.1323	-39.1959	0.1949	47.2950

See! It is identical

Verifying that  $P_w^{-1}$  and  $\hat{Q}_{LQG}$  are the same

Qr =

34.2163	-0.5659	-40.0650	0.5563
-0.5659	33.5834	0.6821	-39.3342
-40.0650	0.6821	48.2812	-0.6948
0.5563	-39.3342	-0.6948	47.4291

ans =

34.2163	-0.5659	-40.0650	0.5563
-0.5659	33.5834	0.6821	-39.3342
-40.0650	0.6821	48.2812	-0.6948
0.5563	-39.3342	-0.6948	47.4291

See! It is identical

Now verifying properties of H Infinity Balanced Truncation....

Verifying that  $Q_v^{-1}$  and  $\hat{P}_H_\infty$  are the same

Pr =

34.7539	0.1653	-40.6286	-0.1056
0.1653	34.0341	-0.2196	-39.8539
-40.6286	-0.2196	48.8848	0.1541
-0.1056	-39.8539	0.1541	48.0253

ans =

34.7539	0.1653	-40.6286	-0.1056
0.1653	34.0341	-0.2196	-39.8539
-40.6286	-0.2196	48.8848	0.1541
-0.1056	-39.8539	0.1541	48.0253

See! It is identical

Verifying that  $P_w^{-1}$  and  $\hat{Q}_H_\infty$  are the same

Qr =

```
34.6392 -0.4389 -40.5242 0.4317
-0.4389 34.1515 0.5279 -39.9617
-40.5242 0.5279 48.7845 -0.5377
0.4317 -39.9617 -0.5377 48.1294
```

ans =

```
34.6392 -0.4389 -40.5242 0.4317
-0.4389 34.1515 0.5279 -39.9617
-40.5242 0.5279 48.7845 -0.5377
0.4317 -39.9617 -0.5377 48.1294
```

See! It is identical

Now verifying properties of positive-realness preserving interpolation (V-type)....

Verifying that  $Q_v^{-1}$  and  $\hat{P}_{PR}$  are the same

Qvi =

```
78.8900 -16.3834 -87.7020 17.6021
-16.3834 63.3069 17.2048 -71.4098
-87.7020 17.2048 99.5050 -18.6180
17.6021 -71.4098 -18.6180 82.4881
```

ans =

```
78.8900 -16.3834 -87.7020 17.6021
-16.3834 63.3069 17.2048 -71.4098
-87.7020 17.2048 99.5050 -18.6180
17.6021 -71.4098 -18.6180 82.4881
```

See! It is identical  
Now checking if it is passive

ans =

logical

1

See! It is passive  
Now let us see if the second realization is passive

ans =

logical

1

See! It is passive  
Now let us see if it satisfies the interpolation conditions

ans =

0.0940	0.1523
-0.0933	0.1756

ans =

0.0940	0.1523
--------	--------

-0.0933 0.1756

ans =

0.0829 0.1304  
-0.0658 0.1615

ans =

0.0829 0.1304  
-0.0658 0.1615

See! It satisfy interpolation conditions

Now see the Hankel singular values of these two realizations to verify these two are identical

Hankel\_singular\_values\_of\_Realization\_1 =

0.2411  
0.2134  
0.0562  
0.0020

Hankel\_singular\_values\_of\_Realization\_2 =

0.2411  
0.2134  
0.0562  
0.0020

See! These two are identical models

Now verifying properties of positive-realness preserving interpolation (W-type)....

Verifying that  $P_w^{-1}$  and  $\hat{Q}_{PR}$  are the same

Pwi =

67.8088	-17.5075	-76.0918	18.1114
-17.5075	74.2142	18.8456	-82.8113
-76.0918	18.8456	87.2517	-19.5897
18.1114	-82.8113	-19.5897	94.4979

ans =

67.8088	-17.5075	-76.0918	18.1114
-17.5075	74.2142	18.8456	-82.8113
-76.0918	18.8456	87.2517	-19.5897
18.1114	-82.8113	-19.5897	94.4979

See! It is identical

Now checking if it is passive

ans =

logical

1

See! It is passive

Now let us see if the second realization is passive

ans =

logical

1

See! It is passive

Now let us see if it satisfies the interpolation conditions

ans =

0.0940 0.1523

-0.0933 0.1756

ans =

0.0940 0.1523

-0.0933 0.1756

ans =

0.0829 0.1304

-0.0658 0.1615

ans =

0.0829 0.1304

-0.0658 0.1615

See! It satisfy interpolation conditions

Now see the Hankel singular values of these two realizations to verify these two are identical

Hankel\_singular\_values\_of\_Realization\_1 =

0.2411

0.2134

0.0562

0.0020

Hankel\_singular\_values\_of\_Realization\_2 =

0.2411

0.2134

0.0562

0.0020

See! These two are identical models

Now verifying properties of Positive-real Balanced Truncation....

Starting with Intrusive Positive-real Balanced Truncation....

Verifying that Intrusive PRBT produced a passive model

ans =

logical

1

It is indeed passive

Now checking the (HANKEL-LIKE) singular values

ans =

0.5727

0.3606

Now moving to Non-intrusive Positive-real Balanced Truncation....

Verifying that Non-intrusive PRBT produced a passive model

ans =

logical

1

It is indeed passive

ans =

0.5733

0.3686

Now checking the (HANKEL-LIKE) singular values

These are close to that of the ROM produced by Intrusive PRBT

Now verifying properties of bounded-realness preserving interpolation (V-type)....

Verifying that  $Q_v^{-1}$  and  $\hat{P}_{BR}$  are the same

Qvi =

```
37.9119 -0.3319 -44.1074 0.2334
-0.3319 39.4810 0.4342 -45.7824
-44.1074 0.4342 52.7317 -0.3266
0.2334 -45.7824 -0.3266 54.5598
```

ans =

```
37.9119 -0.3319 -44.1074 0.2334
-0.3319 39.4810 0.4342 -45.7824
-44.1074 0.4342 52.7317 -0.3266
0.2334 -45.7824 -0.3266 54.5598
```

See! It is identical

Now checking if it is passive

ans =

logical

1

See! It is passive

Now let us see if the second realization is passive

Now checking if it is passive

ans =

logical

1

See! It is passive

Now let us see if it satisfies the interpolation conditions

ans =

0.0940	0.1523
-0.0933	0.1756

ans =

0.0940	0.1523
-0.0933	0.1756

ans =

0.0829	0.1304
-0.0658	0.1615

ans =

0.0829	0.1304
-0.0658	0.1615

See! It satisfy interpolation conditions

Now see the Hankel singular values of these two realizations to verify these two are identical

Hankel\_singular\_values\_of\_Realization\_1 =

0.2170  
0.1807  
0.0182  
0.0052

Hankel\_singular\_values\_of\_Realization\_2 =

0.2170  
0.1807  
0.0182  
0.0052

See! These two are identical models

Now verifying properties of bounded-realness preserving interpolation (W-type)....

Verifying that  $P_w^{-1}$  and  $\hat{Q}_{BR}$  are the same

Pwi =

38.3232	0.9446	-44.5156	-0.9414
0.9446	39.0777	-1.1100	-45.3838
-44.5156	-1.1100	53.1467	1.1346
-0.9414	-45.3838	1.1346	54.1559

ans =

38.3232	0.9446	-44.5156	-0.9414
0.9446	39.0777	-1.1100	-45.3838
-44.5156	-1.1100	53.1467	1.1346

-0.9414 -45.3838 1.1346 54.1559

See! It is identical

Now checking if it is passive

ans =

logical

1

See! It is passive

Now let us see if the second realization is passive

ans =

logical

1

See! It is passive

Now let us see if it satisfies the interpolation conditions

ans =

0.0940 0.1523

-0.0933 0.1756

ans =

```
0.0940    0.1523
-0.0933   0.1756
```

ans =

```
0.0829    0.1304
-0.0658   0.1615
```

ans =

```
0.0829    0.1304
-0.0658   0.1615
```

See! It satisfy interpolation conditions

Now see the Hankel singular values of these two realizations to verify these two are identical

Hankel\_singular\_values\_of\_Realization\_1 =

```
0.2170
0.1807
0.0182
0.0052
```

Hankel\_singular\_values\_of\_Realization\_2 =

```
0.2170
0.1807
0.0182
```

0.0052

See! These two are identical models

Now verifying properties of Bounded-real Balanced Truncation....

Starting with Intrusive Bounded-real Balanced Truncation....

Verifying that Intrusive BRBT produced a passive model

ans =

logical

1

It is indeed passive

Now checking the (HANKEL-LIKE) singular values

ans =

0.2377

0.1957

Now moving to Non-intrusive Bounded-real Balanced Truncation....

Verifying that Non-intrusive BRBT produced a passive model

ans =

logical

1

It is indeed passive

ans =

0.2385

0.1960

Now checking the (HANKEL-LIKE) singular values

These are close to that of the ROM produced by Intrusive BRBT

Now verifying properties of minimum phase preserving interpolation (Zero Placement)...

Verifying if the zeros are at the mirror images of the interpolation points

ans =

-0.7000

-0.7000

-0.5000

-0.5000

See! It is minimum phase with zeros at the mirror images of the interpolation points

Now let us see if it satisfies the interpolation conditions

ans =

0.0940 0.1523

-0.0933 0.1756

ans =

0.0940 0.1523

-0.0933 0.1756

ans =

0.0829	0.1304
-0.0658	0.1615

ans =

0.0829	0.1304
-0.0658	0.1615

See! It satisfy interpolation conditions

Now verifying properties of Self-weighted Balanced Truncation....

Starting with Intrusive Self-weighted Balanced Truncation....

Verifying that SWBT produced a minimum phase model

ans =

-2.6489
-4.0513

It is indeed minimum phase

Now checking the (HANKEL-LIKE) singular values

ans =

1.4069
0.6847

Now moving to Non-intrusive SWBT....

Verifying that Non-intrusive SWBT produced a minimum phase model

ans =

-2.5429

-3.5547

It is indeed minimum phase

Now checking the (HANKEL-LIKE) singular values

ans =

1.4892

0.7028

These are close to that of the ROM produced by Intrusive SWBT

Now verifying properties of Balanced Stochastic Truncation....

Starting with Intrusive Balanced Stochastic Truncation....

Verifying that BST produced a minimum phase model

ans =

-2.6489

-4.0513

It is indeed minimum phase

Now checking the (HANKEL-LIKE) singular values

ans =

0.8151

0.5650

Verifying that Non-intrusive BST produced a minimum phase model

ans =

-2.5421

-3.5553

It is indeed minimum phase

Now checking the (HANKEL-LIKE) singular values

ans =

0.8302

0.5750

These are close to that of the ROM produced by Intrusive BST

## References

- [1] I. V. Gosea, S. Gugercin, C. Beattie, Data-driven balancing of linear dynamical systems, *SIAM Journal on Scientific Computing* 44 (1) (2022) A554–A582.
- [2] U. Zulfiqar, Compression and distillation of data quadruplets in non-intrusive reduced-order modeling, *arXiv preprint arXiv:2501.16683* (2025).
- [3] S. Reiter, I. V. Gosea, S. Gugercin, Generalizations of data-driven balancing: What to sample for different balancing-based reduced models, *arXiv preprint arXiv:2312.12561* (2023).

- [4] P. Benner, Z. Bujanović, P. Kürschner, J. Saak, RADI: A low-rank ADI-type algorithm for large scale algebraic riccati equations, *Numerische Mathematik* 138 (2018) 301–330.
- [5] K. Gallivan, A. Vandendorpe, P. Van Dooren, Sylvester equations and projection-based model reduction, *Journal of Computational and Applied Mathematics* 162 (1) (2004) 213–229.
- [6] C. A. Beattie, S. Gugercin, et al., Model reduction by rational interpolation, *Model Reduction and Approximation* 15 (2017) 297–334.
- [7] A. Mayo, A. C. Antoulas, A framework for the solution of the generalized realization problem, *Linear Algebra and Its Applications* 425 (2-3) (2007) 634–662.
- [8] T. Wolf,  $\mathcal{H}_2$  pseudo-optimal model order reduction, Ph.D. thesis, Technische Universität München (2014).
- [9] M. S. Tombs, I. Postlethwaite, Truncated balanced realization of a stable non-minimal state-space system, *International Journal of Control* 46 (4) (1987) 1319–1330.
- [10] B. Moore, Principal component analysis in linear systems: Controllability, observability, and model reduction, *IEEE Transactions on Automatic Control* 26 (1) (1981) 17–32.
- [11] E. Jonckheere, L. Silverman, A new set of invariants for linear systems—application to reduced order compensator design, *IEEE Transactions on Automatic Control* 28 (10) (1983) 953–964.
- [12] D. Mustafa, K. Glover, Controller reduction by  $\mathcal{H}_\infty$ -balanced truncation, *IEEE Transactions on Automatic Control* 36 (6) (1991) 668–682.
- [13] M. Green, Balanced stochastic realizations, *Linear Algebra and Its Applications* 98 (1988) 211–247.

- [14] J. R. Phillips, L. Daniel, L. M. Silveira, Guaranteed passive balancing transformations for model order reduction, *IEEE Transactions on Computer-Aided Design of Integrated Circuits and Systems* 22 (8) (2003) 1027.
- [15] L. Pernebo, L. Silverman, Model reduction via balanced state space representations, *IEEE Transactions on Automatic Control* 27 (2) (2003) 382–387.
- [16] K. Zhou, Frequency-weighted  $\mathcal{L}_\infty$  norm and optimal hankel norm model reduction, *IEEE Transactions on Automatic Control* 40 (10) (1995) 1687–1699.
- [17] U. Desai, D. Pal, A transformation approach to stochastic model reduction, *IEEE Transactions on Automatic Control* 29 (12) (1984) 1097–1100.
- [18] T. Wolf, H. K. Panzer, The adi iteration for lyapunov equations implicitly performs  $\mathcal{H}_2$  pseudo-optimal model order reduction, *International Journal of Control* 89 (3) (2016) 481–493.
- [19] P. Benner, P. Kürschner, J. Saak, Efficient handling of complex shift parameters in the low-rank cholesky factor ADI method, *Numerical Algorithms* 62 (2013) 225–251.
- [20] M. I. Ahmad, Krylov subspace techniques for model reduction and the solution of linear matrix equations, Ph.D. thesis, Imperial College London (2011).
- [21] C. Bertram, H. Faßbender, On a family of low-rank algorithms for large-scale algebraic riccati equations, *Linear Algebra and Its Applications* 687 (2024) 38–67.
- [22] W. K. Gawronski, *Dynamics and control of structures: A modal approach*, Springer Science & Business Media, 2004.